

Nonlinear spectroscopy by multiresonant four-wave mixing

J-L. Oudar* and Y. R. Shen

*Materials and Molecular Research Division, Lawrence Berkeley Laboratory, University of California, Berkeley, California 94720
and Department of Physics, University of California, Berkeley, California 94720*

(Received 14 January 1980)

Four-wave mixing processes with double and triple resonances are discussed in detail. Explicit expressions for the resonant nonlinear susceptibilities of various cases are derived. It is shown that in some cases, four-wave mixing can yield a spectrum with reduced inhomogeneous broadening. Possible applications of multiresonant four-wave mixing as a spectroscopic technique are considered. They include high-resolution spectroscopy, deduction of transition matrix elements, study of transitions between excited states, measurement of longitudinal relaxation times, distinction between resonant Raman scattering and resonant fluorescence, etc. Selective polarization arrangement allows us to suppress the nonresonant background, separately measure the real and imaginary parts of the resonant nonlinear susceptibility, minimize the effects of absorption and laser intensity fluctuations, and greatly enhance the signal-to-noise ratio.

I. INTRODUCTION

Four-wave mixing is a well-known nonlinear optical effect.¹ It describes a mixing process in which three propagating light waves interact nonlinearly in a medium and generate a fourth wave. The third-order nonlinear susceptibility that governs the process should naturally exhibit resonances which are characteristic of the medium. They can be probed through the resonant enhancement of the four-wave mixing output. Thus, the process can be used as a tool for spectroscopic studies.² With the recent advances of tunable lasers, it is being rapidly developed into an important practical spectroscopic technique for many applications including chemical analysis, combustion research, studies of material properties, etc. The most important advantages of this technique over other techniques are its capability for high-resolution spectroscopic study, for elimination of strong fluorescence background, and for time-resolving measurements of ultrafast dynamic properties.

In most four-wave mixing experiments reported in the literatures, single resonances of the third-order nonlinear susceptibility are usually probed and studied.² Singly resonant four-wave mixing has the merit that the experimental arrangement is relatively simple and interpretation of the results is often straightforward. It generally yields the kind of spectroscopic information one would obtain from one-photon or two-photon transition measurements. Then, similar to resonant Raman scattering versus ordinary Raman scattering,³ four-wave mixing with double or triple resonances should be able to yield more selective spectroscopic information. In addition to the resonant frequencies, the dipole matrix elements between selective states can, in principle, be deduced. Extremely

strong resonant enhancement is of course also expected in doubly or triply resonant four-wave mixing, as has been demonstrated in recent experiments.⁴ Druet *et al.* have recently shown that it is also possible to obtain Doppler-free spectra with doubly and triply resonant four-wave mixing.⁵

In this paper, we give a more thorough discussion on the various problems involved in doubly and triply resonant four-wave mixing processes. We begin by deriving in Sec. II the expressions for third-order nonlinear susceptibilities under different resonant conditions. Both one-photon and two-photon resonances are explicitly displayed, including a predicted two-photon resonance between two excited states. Since real absorption occurs in resonant four-wave mixing, the nonlinear susceptibilities may consist of a part involving only transverse relaxation and a part involving also longitudinal relaxation. The latter often dominates if the longitudinal relaxation time is much longer than the transverse relaxation time.

The resonant spectrum of a singly resonant third-order susceptibility is usually dominated by inhomogeneous broadening. This is not the case with double and triple resonances.⁵ Whenever there is a product of two resonant denominators with damping constants of opposite signs, the inhomogeneous broadening of the corresponding resonant line of the nonlinear susceptibility can be greatly reduced. This can be considered as a generalization of the saturation spectroscopy.⁶ We discuss in Sec. III how the Doppler-free spectrum can be obtained by doubly or triply resonant four-wave mixing, and extend the consideration of Druet *et al.* to ions or molecules in solids.

The output of four-wave mixing in doubly and triply resonant cases is often complicated by absorption at the pump frequencies and/or the out-

put frequency. Absorption reduces the active length of interaction, limits the pump intensity, and broadens the phase-matching peak. Moreover, the dispersion of absorption near resonance distorts the resonant structure of four-wave mixing and makes the four-wave mixing spectrum difficult to interpret. We discuss in Sec. IV how the output depends on resonances, absorptions, and polarizations of the four waves, and show that it is possible to eliminate the dispersion effect of absorption by polarization measurements.⁷

Resonant four-wave mixing can provide detailed spectroscopic information about various transitions. In Sec. V, we consider a number of physical problems on which the application of resonant four-wave mixing spectroscopy is most attractive. We limit the discussion to the steady-state case. It is seen that from the resonant four-wave mixing spectra both the transition frequencies and the transition matrix elements can be deduced. In some cases, spectra with reduced inhomogeneous broadening can be obtained. This is most interesting for studies of Raman transitions between excited states as they cannot be achieved by other techniques. Doubly or triply resonant mixing with an induced population change also leads to a measurement of the longitudinal relaxation times for various states.⁸ Then, by observing the difference between different but related resonant four-wave mixing spectra, one should be able to distinguish resonant Raman scattering and resonant fluorescence,⁹ which has been a controversy in recent years.

Finally, in Sec. VI, we give some considerations to the practical experimental problems. The incoherent scattering and luminescence background can be minimized by spatial and frequency filtering, and in some cases, by time discrimination. The nonresonant background of the resonant mixing spectrum is most effectively suppressed by induced gain or loss spectroscopy¹⁰ or by polarization arrangement.^{7,11} The signal-to-noise ratio of four-wave mixing is derived. In most cases with pulsed laser sources, the noise arises mainly from laser intensity fluctuations. With the polarization-sensitive four-wave mixing,⁷ however, this type of noise is practically eliminated.

II. NONLINEAR POLARIZATIONS AND NONLINEAR SUSCEPTIBILITIES FOR FOUR-WAVE MIXING

Four-wave mixing is governed by a third-order nonlinear polarization $\tilde{P}^{(3)}$. In the steady-state case, $\tilde{P}^{(3)}$ is characterized by a nonlinear susceptibility $\tilde{\chi}^{(3)}$:

$$\tilde{P}^{(3)}(\omega_4) = \tilde{\chi}^{(3)}(\omega_4 = \omega_1 + \omega_2 + \omega_3) : \tilde{E}(\omega_1)\tilde{E}(\omega_2)\tilde{E}(\omega_3). \quad (1)$$

Using the density-matrix formalism,¹² one can find $\tilde{\chi}^{(3)}$ from the perturbation expansion in a straightforward way. There are, in general, 48 terms in the expression of $\tilde{\chi}^{(3)}$.¹³ In many physical cases, however, only the resonant dispersions of $\tilde{\chi}^{(3)}$ are of interest. One can write $\tilde{\chi}^{(3)}$ as

$$\tilde{\chi}^{(3)} = \tilde{\chi}_{NR}^{(3)} + \tilde{\chi}_R^{(3)}, \quad (2)$$

where $\tilde{\chi}_{NR}^{(3)}$ and $\tilde{\chi}_R^{(3)}$ are, respectively, the nonresonant and resonant parts of $\tilde{\chi}^{(3)}$. The number of terms in $\tilde{\chi}_R^{(3)}$ is then greatly reduced from 48. In this paper, we shall only concern ourselves with the doubly and triply resonant cases.

In dealing with resonances, the damping coefficients for the resonances are important. In the density-matrix formalism, damping relaxation of an off-diagonal element $\rho_{nn'}$ can be written as¹²

$$\left(\frac{\partial \rho_{nn'}}{\partial t}\right)_{\text{damping}} = -\Gamma_{nn'}\rho_{nn'}. \quad (3)$$

The inverse of the damping constant $\Gamma_{nn'} = \Gamma_{n'n}$ is the transverse relaxation time or dephasing time $(T_2)_{nn'}$ for transition between states $|n\rangle$ and $|n'\rangle$. The relaxation of the diagonal elements is governed by

$$\begin{aligned} \left(\frac{\partial \rho_{nn}}{\partial t}\right)_{\text{damping}} &= -\sum_{n'} \gamma_{n'n}\rho_{nn} + \sum_{n'} \gamma_{nn'}\rho_{n'n'} \\ &= -\sum_{n'} \gamma_{n'n}(\rho_{nn} - \rho_{nn}^0) \\ &\quad + \sum_{n'} \gamma_{nn'}(\rho_{n'n'} - \rho_{n'n'}^0), \end{aligned} \quad (4)$$

where $\gamma_{nn'}$ is the transition rate from $|n'\rangle$ to $|n\rangle$ resulting from random fluctuations and ρ_{nn}^0 is the population in $|n\rangle$ at thermal equilibrium. As it stands, only when we have an effective two-level system can we rigorously transform Eq. (4) into

$$\begin{aligned} \left(\frac{\partial \rho_{nn}}{\partial t}\right)_{\text{damping}} &= -\Gamma_{nn}(\rho_{nn} - \rho_{nn}^0) \\ &= -(\rho_{nn} - \rho_{nn}^0)/T_{1n}. \end{aligned} \quad (5)$$

In general, in a multilevel system with all levels participating in the relaxation of excess population in $|n\rangle$, the concept of having a longitudinal relaxation time for $|n\rangle$ does not hold. In special cases, however, Eq. (5) can be considered as a good approximation of Eq. (4). This happens, for exam-

ple, when relaxation of population into $\langle n |$ is negligible, [i.e., the term $\sum_{n'} \gamma_{nn'} (\rho_{n'n'} - \rho_{n'n'}^0)$ in Eq. (4) can be neglected] as is often the case for optically excited states. For ground states, on the other hand, only in limited cases can the relaxation of ρ_{gg} back to ρ_{gg}^0 be approximated by

$$\left(\frac{\partial}{\partial t} \rho_{gg} \right)_{\text{damping}} = - \frac{(\rho_{gg} - \rho_{gg}^0)}{T_{1g}}. \quad (6)$$

This is the case, for example, when one relaxation route from $\langle n |$ to $\langle g |$ dominates in the relaxation process.

While the approximations of Eqs. (5) and (6) should be justified separately for individual cases, we shall assume for simplicity in the following discussion that they do hold. We consider here only the doubly and triply resonant four-wave mixing processes.

A. Doubly resonant four-wave mixing

We assume only two input laser frequencies ω_1 and ω_2 , and consider the various doubly resonant cases shown in Fig. 1. We also assume that only the ground state $\langle g |$ is initially populated. In Figs. 1(a)–1(d), the output frequency is $2\omega_1 - \omega_2$. Following the density-matrix formalism or Yee and Gustafson's diagrammatic technique,¹⁴ we find for Figs. 1(a), 1(b), 1(c), and 1(d), respectively,

$$\begin{aligned} [\chi_R^{(3)}(\omega_3 = \omega_1 - \omega_2 + \omega_1)]_{ijkl} = & - \frac{Ne^4}{\hbar^3} \sum_m \left(\frac{\langle g | r_i | m \rangle \langle m | r_j | g' \rangle}{2\omega_1 - \omega_2 - \omega_{mg}} + \frac{\langle g | r_j | m \rangle \langle m | r_i | g' \rangle}{2\omega_1 - \omega_2 + \omega_{mg'}} \right) \\ & \times \frac{\langle g' | r_k | n \rangle \langle n | r_l | g \rangle \rho_{gg}^0}{(\omega_1 - \omega_{ng} + i\Gamma_{ng})(\omega_1 - \omega_2 - \omega_{g'g} + i\Gamma_{g'g})} + \dots, \end{aligned} \quad (7a)$$

$$\begin{aligned} [\chi_R^{(3)}(\omega_3 = \omega_1 - \omega_2 + \omega_1)]_{ijkl} = & - \frac{Ne^4}{\hbar^3} \sum_m \frac{\langle g | r_i | m' \rangle}{2\omega_1 - \omega_2 - \omega_{n'g} + i\Gamma_{n'g}} \\ & \times \left(\frac{\langle n' | r_j | m \rangle \langle m | r_k | n \rangle}{\omega_1 - \omega_2 - \omega_{mg}} \cdot \frac{\langle n' | r_l | m \rangle \langle m | r_j | n \rangle}{2\omega_1 - \omega_{mg}} \right) \frac{\langle n | r_i | g \rangle \rho_{gg}^0}{\omega_1 - \omega_{ng} + i\Gamma_{ng}} + \dots, \end{aligned} \quad (7b)$$

$$\begin{aligned} [\chi_R^{(3)}(\omega_3 = \omega_1 - \omega_2 + \omega_1)]_{ijkl} = & - \frac{Ne^4}{\hbar^3} \sum_m \frac{\langle g | r_i | n' \rangle \langle n' | r_j | g' \rangle}{(2\omega_1 - \omega_2 - \omega_{n'g} + i\Gamma_{n'g})(\omega_1 - \omega_2 - \omega_{g'g} + i\Gamma_{g'g})} \\ & \times \left(\frac{\langle g' | r_k | m \rangle \langle m | r_l | g \rangle}{\omega_1 - \omega_{mg}} + \frac{\langle g' | r_l | m \rangle \langle m | r_k | g \rangle}{-\omega_2 - \omega_{mg}} \right) \rho_{gg}^0 + \dots, \end{aligned} \quad (7c)$$

$$\begin{aligned} [\chi_R^{(3)}(\omega_3 = \omega_1 - \omega_2 + \omega_1)]_{ijkl} = & - \frac{Ne^4}{\hbar^3} \sum_m \frac{\langle m | r_i | n' \rangle \langle n' | r_j | g \rangle \langle g | r_k | n \rangle \langle n | r_l | m \rangle}{(2\omega_1 - \omega_2 - \omega_{n'm})(\omega_1 - \omega_2 - \omega_{n'n} + i\Gamma_{n'n})} \\ & \times \left(\frac{1}{\omega_1 - \omega_{n'g} + i\Gamma_{n'g}} - \frac{1}{\omega_2 - \omega_{ng} - i\Gamma_{ng}} \right) \rho_{gg}^0 + \dots, \end{aligned} \quad (7d)$$

where ellipses denote terms with j and l interchanged. Resonances are explicitly shown in the above expressions by the frequency denominators with damping constants. The physical processes governed by

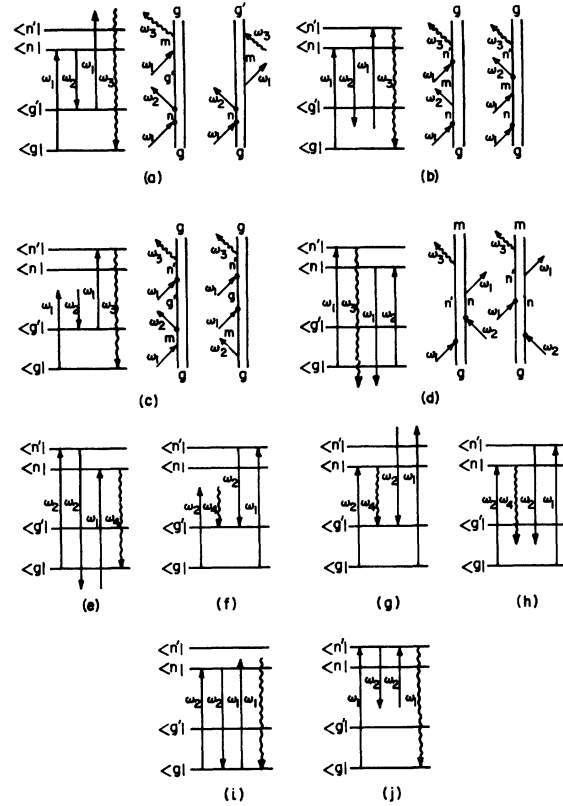


FIG. 1. Schematic representation of various doubly resonant four-wave mixing processes. In (a)–(d) the degenerate cases are explicitly shown using the double-path diagrams (Ref. 14). There are also two degenerate cases in (e)–(h) and eight in (i) and (j).

the nonlinear susceptibilities in Eqs. (7a)–(7c) are often known as doubly resonant CARS (coherent anti-Stokes Raman scattering). Equation (7d) shows, however, that the same four-wave mixing process can be used to probe resonant transition between excited states when $(\omega_1 - \omega_2) \cong \omega_{n'n}$,¹³ if $\Gamma_{ng} + \Gamma_{n'g} \neq \Gamma_{n'n}$. The strength of this resonance is greatly enhanced as ω_1 and ω_2 approach resonances. It depends critically on the corresponding damping constants and hence the damping mechanism. A model calculations of this resonance is given in Ref. 13.

Similarly, we obtain for Figs. 1(e), 1(f), 1(g), and 1(h), respectively, at the output frequency $2\omega_2 - \omega_1$

$$\chi_R^{(3)}(\omega_4 = \omega_2 - \omega_1 + \omega_2)_{ijkl} = -\frac{Ne^4}{\hbar^3} \sum_m \frac{\langle g|r_i|n \rangle}{2\omega_2 - \omega_1 - \omega_{ng} + i\Gamma_{ng}} \times \left(\frac{\langle n|r_j|m \rangle \langle m|r_k|n' \rangle}{\omega_2 - \omega_1 - \omega_{mg}} + \frac{\langle n|r_k|m \rangle \langle m|r_j|n' \rangle}{2\omega_2 - \omega_{mg}} \right) \frac{\langle n'|r_l|g \rangle \rho_{gg}^0}{\omega_2 - \omega_{n'g} + i\Gamma_{n'g}} + \dots, \quad (7e)$$

$$\chi_R^{(3)}(\omega_4 = \omega_2 - \omega_1 + \omega_2)_{ijkl} = -\frac{Ne^4}{\hbar^3} \sum_m \left(\frac{\langle g'|r_i|m \rangle \langle m|r_j|g \rangle}{2\omega_2 - \omega_1 - \omega_{mg'}} - \frac{\langle g'|r_j|m \rangle \langle m|r_i|g \rangle}{2\omega_2 - \omega_1 + \omega_{mg'}} \right) \times \frac{\langle g|r_k|n' \rangle \langle n'|r_l|g' \rangle \rho_{gg}^0}{(\omega_1 - \omega_2 - \omega_{g'g} - i\Gamma_{g'g})(\omega_1 - \omega_{n'g} - i\Gamma_{n'g})} + \dots, \quad (7f)$$

$$\chi_R^{(3)}(\omega_4 = \omega_2 - \omega_1 + \omega_2)_{ijkl} = -\frac{Ne^4}{\hbar^3} \sum_m \frac{\langle g'|r_i|n \rangle \langle n|r_j|g \rangle}{(2\omega_2 - \omega_1 - \omega_{ng'} + i\Gamma_{ng'})(\omega_1 - \omega_2 - \omega_{g'g} - i\Gamma_{g'g})} \times \left(\frac{\langle g|r_k|m \rangle \langle m|r_i|g' \rangle}{\omega_1 - \omega_{mg}} - \frac{\langle g|r_i|m \rangle \langle m|r_k|g' \rangle}{\omega_2 + \omega_{mg}} \right) \rho_{gg}^0 + \dots, \quad (7g)$$

$$\chi_R^{(3)}(\omega_4 = \omega_2 - \omega_1 + \omega_2)_{ijkl} = -\frac{Ne^4}{\hbar^3} \sum_m \frac{\langle m|r_i|n \rangle \langle n|r_j|g \rangle \langle g|r_k|n' \rangle \langle n'|r_l|m \rangle}{(\omega_1 - 2\omega_2 - \omega_{mn})(\omega_1 - \omega_2 - \omega_{n'n} - i\Gamma_{n'n})} \times \left(\frac{1}{\omega_1 - \omega_{n'g} - i\Gamma_{n'g}} - \frac{1}{\omega_2 - \omega_{ng} + i\Gamma_{ng}} \right) \rho_{gg}^0 + \dots, \quad (7h)$$

where the ellipses represent terms with j and l interchanged. Again, the nonlinear susceptibility in Eq. (7h) governs the physical process that probes the resonance between excited states. As seen in Eqs. (7a)–(7h), all resonances involve only transverse dephasing relaxation. This is not the case if the output frequency is ω_1 or ω_2 . We find for Figs. 1(i) and 1(j), respectively, with the output frequency at ω_1 ,

$$\chi_R^{(3)}(\omega_1 = \omega_1 - \omega_2 + \omega_2)_{ijkl} = \frac{Ne^4}{\hbar^3} \sum_m \left[\left(\frac{\langle g|r_i|m \rangle \langle m|r_j|g \rangle}{\omega_1 - \omega_{mg}} + \frac{\langle g|r_j|m \rangle \langle m|r_i|g \rangle}{\omega_1 + \omega_{mg}} \right) \frac{\langle g|r_k|n \rangle \langle n|r_l|g \rangle 2\Gamma_{ng} T_{1g} \rho_{gg}^0}{(\omega_2 - \omega_{ng})^2 + \Gamma_{ng}^2} - \left(\frac{\langle n|r_i|m \rangle \langle m|r_j|n \rangle}{\omega_1 - \omega_{mn}} + \frac{\langle n|r_j|m \rangle \langle m|r_i|n \rangle}{\omega_1 + \omega_{mn}} \right) \frac{\langle n|r_k|g \rangle \langle g|r_l|n \rangle 2\Gamma_{ng} T_{1n} \rho_{gg}^0}{(\omega_2 - \omega_{ng})^2 + \Gamma_{ng}^2} \right], \quad (7i)$$

$$\chi_R^{(3)}(\omega_1 = \omega_1 - \omega_2 + \omega_2)_{ijkl} = \frac{Ne^4}{\hbar^3} \sum_m \frac{\langle g|r_i|n \rangle \langle n|r_j|g \rangle}{(\omega_1 - \omega_{ng} + i\Gamma_{ng})^2} \left(\frac{\langle n|r_k|m \rangle \langle m|r_i|n \rangle}{\omega_1 + \omega_2 - \omega_{mg}} + \frac{\langle n|r_i|m \rangle \langle m|r_k|n \rangle}{\omega_1 - \omega_2 - \omega_{mg}} \right) + \frac{\langle m|r_k|g \rangle \langle g|r_i|m \rangle}{\omega_1 + \omega_2 - \omega_{nm}} + \frac{\langle m|r_i|g \rangle \langle g|r_k|m \rangle}{\omega_1 - \omega_2 - \omega_{nm}} \rho_{gg}^0. \quad (7j)$$

Interchanging ω_1 and ω_2 in Eqs. (7i) and (7j) for $\chi_R^{(3)}(\omega_1 = \omega_1 - \omega_2 + \omega_2)$ yields the expressions for $\chi_R^{(3)}(\omega_2 = \omega_2 - \omega_1 + \omega_1)$. The case of Eq. (7i) involves a double resonance with a real population change and hence the longitudinal relaxation times T_{1g} and T_{1n} . Equation (7j), on the other hand, is a coherent process involving only transverse relaxation.

Four-wave mixing with $2\omega_1$, $2\omega_2$, or $\omega_1 + \omega_2$ at resonances is a simple extension of the above discussion.

B. Triply resonant four-wave mixing

We now consider cases where all the three frequency denominators are near resonances. Again, we assume that there are only two input laser frequencies ω_1 and ω_2 . The relevant processes are shown in Fig. 2. The nonlinear susceptibilities corresponding to Figs. (2a)–(2d), respectively, are

$$\chi_R^{(3)}(\omega_1 = \omega_2 - \omega_2 + \omega_1)_{ijkl} = -\frac{Ne^4}{\hbar^3} \frac{\langle g|r_i|n' \rangle \langle n'|r_j|g' \rangle \langle g'|r_k|n' \rangle \langle n'|r_l|g \rangle \rho_{gg}^0}{(\omega_1 - \omega_{n'g} + i\Gamma_{n'g})^2 (\omega_1 - \omega_2 - \omega_{g'g} + i\Gamma_{g'g})}, \quad (8a)$$

$$\begin{aligned}
[\chi_{\mathbb{R}}^{(3)}(\omega_1 = \omega_2 - \omega_2 + \omega_1)]_{ijkl} &= (Ne^4/\hbar^3) \langle g|r_i|n' \rangle \langle n'|r_j|g \rangle \langle g|r_k|n' \rangle \langle n'|r_l|g \rangle \rho_{\mathbb{E}\mathbb{E}}^0 \\
&\times \{ (\omega_1 - \omega_{n'\mathbb{E}} + i\Gamma_{n'\mathbb{E}})^{-1} (\omega_1 - \omega_2 - \omega_{n'n} + i\Gamma_{n'n})^{-1} [(\omega_2 - \omega_{n\mathbb{E}} - i\Gamma_{n\mathbb{E}})^{-1} - (\omega_1 - \omega_{n'\mathbb{E}} + i\Gamma_{n'\mathbb{E}})^{-1}] \\
&\quad + 2\Gamma_{n\mathbb{E}} T_{\mathbb{E}} (\omega_1 - \omega_{n'\mathbb{E}} + i\Gamma_{n'\mathbb{E}})^{-1} [(\omega_2 - \omega_{n\mathbb{E}})^2 + \Gamma_{n\mathbb{E}}^2]^{-1} \}, \tag{8b}
\end{aligned}$$

$$\begin{aligned}
[\chi_{\mathbb{R}}^{(3)}(\omega_2 = \omega_1 - \omega_1 + \omega_2)]_{ijkl} &= (Ne^4/\hbar^3) \langle g'|r_i|n' \rangle \langle n'|r_j|g \rangle \langle g|r_k|n' \rangle \langle n'|r_l|g' \rangle \rho_{\mathbb{E}\mathbb{E}}^0 \\
&\times \{ [- (\omega_2 - \omega_{n'\mathbb{E}'} + i\Gamma_{n'\mathbb{E}'}) (\omega_1 - \omega_{n'\mathbb{E}} - i\Gamma_{n'\mathbb{E}}) (\omega_1 - \omega_2 - \omega_{\mathbb{E}'\mathbb{E}} - i\Gamma_{\mathbb{E}'\mathbb{E}})]^{-1} \\
&\quad + 2\Gamma_{n'\mathbb{E}'} T_{1n'} (\omega_2 - \omega_{n'\mathbb{E}'} + i\Gamma_{n'\mathbb{E}'})^{-1} [(\omega_1 - \omega_{n'\mathbb{E}})^2 + \Gamma_{n'\mathbb{E}}^2]^{-1} \}, \tag{8c}
\end{aligned}$$

$$\begin{aligned}
[\chi_{\mathbb{R}}^{(3)}(\omega_2 = \omega_2 - \omega_1 + \omega_1)]_{ijkl} &= (Ne^4/\hbar^3) \langle g|r_i|n \rangle \langle n|r_j|g \rangle \langle g|r_k|n' \rangle \langle n'|r_l|g \rangle \rho_{\mathbb{E}\mathbb{E}}^0 \\
&\times \{ (\omega_2 - \omega_{n\mathbb{E}} + i\Gamma_{n\mathbb{E}})^{-1} (\omega_1 - \omega_2 - \omega_{n'n} - i\Gamma_{n'n})^{-1} [(\omega_2 - \omega_{n\mathbb{E}} + i\Gamma_{n\mathbb{E}})^{-1} - (\omega_1 - \omega_{n'\mathbb{E}} - i\Gamma_{n'\mathbb{E}})^{-1}] \\
&\quad + 2\Gamma_{n'\mathbb{E}} T_{\mathbb{E}} (\omega_2 - \omega_{n\mathbb{E}} + i\Gamma_{n\mathbb{E}})^{-1} [(\omega_1 - \omega_{n'\mathbb{E}})^2 + \Gamma_{n'\mathbb{E}}^2]^{-1} \}. \tag{8d}
\end{aligned}$$

Again, in these expressions, various resonances are explicitly shown. That the processes can be divided into two parts is also apparent, a coherent part involving only transverse relaxation and a partially incoherent part with population change involving longitudinal relaxation.

C. Four-wave mixing with three input frequencies

In the literatures, four-wave mixing with three input laser frequencies is seldom discussed.¹⁵ It is, however, an interesting case since three separately tunable laser beams can provide much greater flexibility in four-wave mixing, especially when triple resonances are probed. We consider here only a special case where two of the three frequencies ω_1 and ω'_1 are nearly equal. Then, the most important modification on the nonlinear susceptibilities with two input frequencies is on the terms involving real population change with T_1 relaxation. The factor T_1 should be replaced by $i(\omega_1 - \omega'_1 + i/T_1)^{-1}$ and the factor $i2\Gamma_{n\mathbb{E}}/[(\omega_1 - \omega_{n\mathbb{E}})^2 + \Gamma_{n\mathbb{E}}^2]$ should be replaced by $[(\omega_1 - \omega_{n\mathbb{E}} - i\Gamma_{n\mathbb{E}})^{-1} - (\omega'_1 - \omega_{n\mathbb{E}} + i\Gamma_{n\mathbb{E}})^{-1}]$ (or with ω_1 and ω'_1 interchanged). For example, in the case of triple resonances, Eqs. (8c) and (8d) become, respectively,

$$\begin{aligned}
[\chi_{\mathbb{R}}^{(3)}(\omega'_2 = \omega_1 - \omega'_1 + \omega_2)]_{ijkl} &= (Ne^4/\hbar^3) \langle g'|r_i|n' \rangle \langle n'|r_j|g \rangle \langle g|r_k|n' \rangle \langle n'|r_l|g' \rangle \rho_{\mathbb{E}\mathbb{E}}^0 \\
&\times \{ [(\omega'_2 - \omega_{n'\mathbb{E}'} + i\Gamma_{n'\mathbb{E}'}) (\omega'_1 - \omega_2 - \omega_{\mathbb{E}'\mathbb{E}} - i\Gamma_{\mathbb{E}'\mathbb{E}}) (\omega_1 - \omega_{n'\mathbb{E}} - i\Gamma_{n'\mathbb{E}})]^{-1} \\
&\quad + (\omega'_2 - \omega_{n'\mathbb{E}'} + i\Gamma_{n'\mathbb{E}'})^{-1} (\omega_1 - \omega'_1 + i/T_{1n'})^{-1} [(\omega_1 - \omega_{n'\mathbb{E}} - i\Gamma_{n'\mathbb{E}})^{-1} - (\omega'_1 - \omega_{n'\mathbb{E}} + i\Gamma_{n'\mathbb{E}})^{-1}] \}, \tag{9a}
\end{aligned}$$

$$\begin{aligned}
[\chi_{\mathbb{R}}^{(3)}(\omega'_2 = \omega_2 - \omega'_1 + \omega_1)]_{ijkl} &= (Ne^4/\hbar^3) \langle g|r_i|n \rangle \langle n|r_j|g \rangle \langle g|r_k|n' \rangle \langle n'|r_l|g \rangle \rho_{\mathbb{E}\mathbb{E}}^0 \\
&\times \{ (\omega'_2 - \omega_{n\mathbb{E}} + i\Gamma_{n\mathbb{E}})^{-1} (\omega'_1 - \omega_2 - \omega_{n'n} - i\Gamma_{n'n})^{-1} [(\omega_2 - \omega_{n\mathbb{E}} + i\Gamma_{n\mathbb{E}})^{-1} - (\omega'_1 - \omega_{n'\mathbb{E}} - i\Gamma_{n'\mathbb{E}})^{-1}] \\
&\quad + (\omega'_2 - \omega_{n\mathbb{E}} + i\Gamma_{n\mathbb{E}})^{-1} (\omega_1 - \omega'_1 + i/T_{\mathbb{E}})^{-1} [(\omega_1 - \omega_{n'\mathbb{E}} - i\Gamma_{n'\mathbb{E}})^{-1} - (\omega'_1 - \omega_{n'\mathbb{E}} + i\Gamma_{n'\mathbb{E}})^{-1}] \}. \tag{9b}
\end{aligned}$$

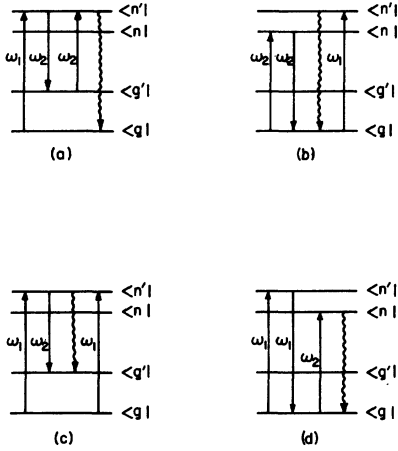


FIG. 2. Schematic representation of various triply resonant four-wave mixing processes. There are four degenerate cases in (b)–(d).

There are also two similar equations for $\chi_R^{(3)}(\omega_2'' = \omega_1' - \omega_1 + \omega_2)$ and $\chi_R^{(3)}(\omega_2'' = \omega_2 - \omega_1 + \omega_1')$ obtained by interchanging ω_1 and ω_1' in Eqs. (9a) and (9b). A similar modification applies to $\chi_R^{(3)}(\omega_1)$ for the

$$[\chi_R^{(3)}(\omega_2'' = \omega_1 - \omega_1' + \omega_2)]_{ijkl} = \frac{Ne^2 \langle g' | r_i | n' \rangle \rho_{n'n'}^{(2)}(\omega_1 - \omega_1') \langle n' | r_j | g' \rangle}{\hbar (\omega_2'' - \omega_{n'g'} + i\Gamma_{n'g'}) E_j(\omega_1) E_k^*(\omega_1')} \quad (10)$$

Now, through population relaxation, other $|m\rangle$ states also become populated, i.e., $\rho_{mm}^{(2)}(\omega_1 - \omega_1') \neq 0$. Should $\rho_{mm}^{(2)}(\omega_1 - \omega_1')$ also contribute to $\chi_R^{(3)}$? Indeed, Eq. (10) should be generalized to

$$[\chi_R^{(3)}(\omega_2'' = \omega_1 - \omega_1' + \omega_2)]_{ijkl} = \frac{Ne^2}{\hbar E_j(\omega_1) E_k^*(\omega_1')} \sum_m \frac{\langle g' | r_i | m \rangle \rho_{mm}^{(2)}(\omega_1 - \omega_1') \langle m | r_j | g' \rangle}{(\omega_2'' - \omega_{mg'} + i\Gamma_{mg'})} \quad (11)$$

The above equation manifests a rather interesting situation: As $\omega_2'' - \omega_{mg'}$, the $\rho_{mm}^{(2)}(\omega_1 - \omega_1')$ is resonantly enhanced. This leads to the unusual triply resonant four-wave mixing depicted in Fig. 3. We can, in general, deduce $\rho_{mm}^{(2)}(\omega_1 - \omega_1')$ from Eq. (4). However, in the case where a particular relaxation route from $|n'\rangle$ to $|m\rangle$ dominates and T_{1m} for $|m\rangle$ is well defined, we can write

$$\begin{aligned} \rho_{mm}^{(2)}(\omega_1 - \omega_1') &= \gamma'_{mn'} \rho_{n'n'}^{(2)}(\omega_1 - \omega_1') / (\omega_1 - \omega_1' + i/T_{1m}) \\ &= \frac{e^2 \gamma'_{mn'} \langle n' | r_j | g \rangle \langle g | r_k | n' \rangle E_j(\omega_1) E_k^*(\omega_1')}{\hbar^2 (\omega_1 - \omega_1' + i/T_{1n'}) (\omega_1 - \omega_1' + i/T_{1m})} \left(\frac{1}{\omega_1 - \omega_{n'g} - i\Gamma_{n'g}} - \frac{1}{\omega_1 - \omega_{n'g} + i\Gamma_{n'g}} \right) \rho_{gg}^0, \end{aligned} \quad (12)$$

where $\gamma'_{mn'}$ is a constant. It is possible to have $|\rho_{mm}^{(2)}(\omega_1 - \omega_1')| > |\rho_{n'n'}^{(2)}(\omega_1 - \omega_1')|$ as $\omega_1 - \omega_1'$. This happens when $T_{1m} > 1/\gamma'_{mn'}$. Thus, the process in Fig. 3 can yield a spectrum of $\chi_R^{(3)}(\omega_2)$ vs $(\omega_1 - \omega_1')$ showing two superimposed Lorentzian lines with halfwidths $T_{1n'}^{-1}$ and T_{1m}^{-1} , respectively. Again, such a resonant spectrum is expected to exhibit no inhomogeneous broadening.

III. EFFECTS OF INHOMOGENEOUS BROADENING ON $\chi_R^{(3)}$

The resonant frequencies of a system often depend on its local environment. For atomic and

doubly resonant cases. As is apparent in Eqs. (9a) and (9b), one clear advantage of having three input frequencies is that we can now vary $\omega_1 - \omega_1'$ to probe a zero-frequency resonance with a T_1^{-1} halfwidth. The triple-resonance condition may, furthermore, selectively enhance, e.g., the $(\omega_1 - \omega_1' + i/T_{1n})^{-1}$ term of Eq. (9a) against the $(\omega_1 - \omega_1' + i/T_{1m})^{-1}$ term of Eq. (9b). In contrast to resonances at finite frequencies, these zero-frequency resonances are not subject to inhomogeneous broadening, and therefore their halfwidths yield directly the T_1 relaxation times of the resonant states. This is fundamentally different from the case discussed in the next section where inhomogeneous broadening is reduced through double or triple resonances with damping constants of opposite signs. We shall give a more explicit description of the proposed measurement of T_1 using this scheme in Sec. V.D.

Physically, terms involving T_1 in $\chi_R^{(3)}$ arise from a population change represented by the diagonal terms of the second-order density matrix $\rho^{(2)}(\omega_1 - \omega_1')$. For example, the second term of Eq. (9a) can be written as

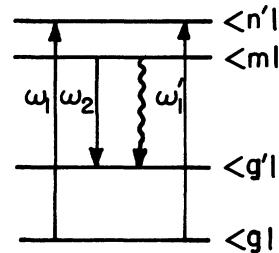


FIG. 3. Special triply resonant four-wave mixing process in which the level $|m\rangle$ is populated through relaxation of excitation.

molecular gases, the resonant frequencies are modified by the Doppler shifts, and for ions in condensed matter, they are modified by the local crystal field. Thus, the effective $\bar{\chi}_R^{(3)}$ must be a weighted average of $\bar{\chi}_R^{(3)}$ over the distribution of the resonant frequencies.

We can assume that the eigenenergies E_i, E_j, \dots of the states $|i\rangle, |j\rangle, \dots$ of the system depend on some local parameters $\alpha, \beta, \gamma, \dots$. Then, the resonant frequencies $(E_i - E_j)/\hbar \equiv \omega_{ij}(\alpha, \beta, \dots)$ are functions of α, β, \dots . If the distribution function $g(\alpha, \beta, \dots)$ for the system is known, the average $\bar{\chi}_R$ can be explicitly written as

$$\langle \bar{\chi}_R^{(3)} \rangle = \int \bar{\chi}_R^{(3)} g(\alpha, \beta, \dots) (d\alpha d\beta, \dots). \quad (13)$$

Clearly, among the various resonant frequency denominators in $\bar{\chi}_R^{(3)}$, the zero-frequency resonances are not affected by the local parameters and can be pulled out of the integral. Therefore, the zero-frequency resonances in Eq. (9) do not suffer inhomogeneous broadening and their half-widths yield directly T_1 .

$$X_R^{(3)} = A_D \int dv g(v) / [\omega_a - \omega_{ij}^0(1 - v/c) \pm i\Gamma_{ij}] [\omega_b - \omega_{kl}^0(1 - v/c) \pm i\Gamma_{kl}], \quad (16)$$

where A_D is a constant independent of v . If we define

$$\nu \equiv v/v_0,$$

$$\xi_a = \xi'_a + i\xi''_a \equiv (c/v_0)(1 - \omega_a/\omega_{ij}^0 \pm i\Gamma_{ij}/\omega_{ij}^0), \quad (17)$$

$$\xi_b = \xi'_b + i\xi''_b \equiv (c/v_0)(1 - \omega_b/\omega_{kl}^0 \pm i\Gamma_{kl}/\omega_{kl}^0),$$

Eq. (12) becomes

$$X_R^{(3)} = K_D \int d\nu e^{-\nu^2/\sqrt{\pi}} (\nu - \xi_a)(\nu - \xi_b), \quad (18)$$

$$K_D = A_D c^2 / v_0^2 \omega_{ij}^0 \omega_{kl}^0.$$

The above integral can be evaluated in terms of the plasma dispersion function¹⁶

$$Z(\xi = \xi' + i\xi'') = \pi^{-1/2} \int_{-\infty}^{\infty} d\nu \frac{e^{-\nu^2}}{(\nu - \xi)} \quad \text{for } \xi'' > 0, \quad (19)$$

which has the properties

$$\begin{aligned} Z(\xi^*) &= -Z^*(-\xi), \\ Z'(\xi) &\equiv \frac{dZ}{d\xi} = -2[1 + \xi Z(\xi)], \\ Z''(\xi) &\equiv \frac{d^2Z}{d\xi^2} = -2[Z(\xi) + \xi Z'(\xi)], \end{aligned} \quad (20)$$

$$Z^*(\xi^*) = \xi' - i\xi'' = Z(\xi) - i2\sqrt{\pi} \exp(-\xi^2),$$

$$Z^*(\xi^*) = \pi^{-1/2} \int_{-\infty}^{\infty} d\nu \frac{e^{-\nu^2}}{(\nu - \xi)} \quad \text{for } \xi'' < 0.$$

The last equation results from the analytical continuity of $Z(\xi)$. We then find that $X_R^{(3)}$ behaves

A. Doppler broadening

The simplest case of inhomogeneous broadening is the case of Doppler broadening in a gas medium. Its effect on $\bar{\chi}_R^{(3)}$ has recently been discussed in great detail by Druet *et al.*⁵ Taking into account the first-order Doppler shift, the resonance frequency is

$$\omega_{ij} = \omega_{ij}^0(1 - v/c), \quad (14)$$

with the particle velocity v being the only local parameter. The function g is simply the Maxwellian distribution

$$g(v) = (1/\sqrt{\pi} v_0) \exp(-v^2/v_0^2). \quad (15)$$

In this case, the averaging can be carried out analytically.

An immediate question one might raise is whether the doubly or triply resonant four-wave mixing spectroscopy can eliminate Doppler broadening. Consider first the doubly resonant cases. Aside from the zero-frequency resonant terms, a typical term of $\bar{\chi}_R^{(3)}$ has the form

differently near the double resonance $\xi'_a = \xi'_b$, depending on the relative signs of ξ''_a and ξ''_b . If ξ''_a and ξ''_b are both positive, then we can write

$$X_R^{(3)} = K_D [Z(\xi_a) - Z(\xi_b)] / (\xi_a - \xi_b), \quad (21)$$

which shows no singularity as $\xi_a \rightarrow \xi_b$. In fact, with $\xi''_a = \xi''_b$, we have $X_R^{(3)} = K_D Z'(\xi_a)$ as $\xi'_a \rightarrow \xi'_b$, and $X_R^{(3)}$ vs ξ'_a has a width more than twice the Doppler width. The same behavior occurs with ξ''_a and ξ''_b both negative. If, however, ξ''_a and ξ''_b have opposite signs, then with the help of the last equation in Eq. (20), we obtain, as $\xi_a \rightarrow \xi_b^*$,

$$X_R^{(3)} = K_D [Z'(\xi_a) \pm i2\sqrt{\pi} e^{-(\xi'_a - i\xi''_a)^2} / (\xi_a - \xi_b)], \quad (22)$$

where $+$ and $-$ correspond to $\xi''_a > 0$ and $\xi''_a < 0$, respectively. The last term in Eq. (22) diverges as $\xi_a \rightarrow \xi_b$. It has a Lorentzian line shape with a halfwidth $\xi''_a + \xi''_b = (c/v_0)(\Gamma_{ij}/\omega_{ij}^0 + \Gamma_{kl}/\omega_{kl}^0)$. In other words, as $\omega_a/\omega_{ij}^0 \rightarrow \omega_b/\omega_{kl}^0$ at double resonance, and if the Doppler width is much larger than the natural widths, $X_R^{(3)}$ vs ω_a/ω_{ij}^0 can be approximated by a Lorentzian with a linewidth given by the sum of the normalized natural linewidths $(\Gamma_{ij}/\omega_{ij}^0 + \Gamma_{kl}/\omega_{kl}^0)$. Thus, a Doppler-free spectrum is obtained. For the various doubly resonant cases in Eq. (7) and Fig. 1, we note that Eqs. (7d), (7g), and (7h) should yield Doppler-free spectra.

The above discussion can be extended to the triply resonant cases. A typical term in the average nonlinear susceptibility $\bar{\chi}_R^{(3)}$ is

$$\begin{aligned}
X_R^{(3)} &= A_T \int d\nu g(\nu) / \left[\omega_a - \omega_{ij}^0 \left(1 - \frac{\nu}{c} \right) \pm i\Gamma_{ij} \right] \left[\omega_b - \omega_{ki}^0 \left(1 - \frac{\nu}{c} \right) \pm i\Gamma_{ki} \right] \left[\omega_c - \omega_{mn}^0 \left(1 - \frac{\nu}{c} \right) \pm i\Gamma_{mn} \right] \\
&= K_T \int d\nu \frac{e^{-\nu^2}}{(\nu - \xi_a)(\nu - \xi_b)(\nu - \xi_c)} \\
&= K_T \left(\frac{F(\xi_a)}{(\xi_a - \xi_b)(\xi_a - \xi_c)} + \frac{F(\xi_b)}{(\xi_b - \xi_a)(\xi_b - \xi_c)} + \frac{F(\xi_c)}{(\xi_c - \xi_a)(\xi_c - \xi_b)} \right), \quad (23)
\end{aligned}$$

with $K_T = A_T c^3 / v_0^3 \omega_{ij}^0 \omega_{ki}^0 \omega_{mn}^0$, $F(\xi) = Z(\xi)$ if $\xi'' > 0$, and $F(\xi) = Z^*(\xi^*)$ if $\xi'' < 0$. At triple resonance $\xi'_a - \xi'_b \simeq \xi'_c$, if ξ'_a , ξ'_b , and ξ'_c all have the same sign, then $X_R^{(3)}$ shows no singularity, and for $\xi'_a = \xi'_b = \xi'_c$, $X_R^{(3)} = K_T Z''(\xi_a) / 2$. The spectrum should exhibit Doppler broadening. On the other hand, if one of the ξ'' , say ξ''_a , has an opposite sign from the others, we obtain as $\xi'_a - \xi'_b \simeq \xi'_c$,

$$X_R^{(3)} = K_T [Z''(\xi_a) / 2 \pm i2\sqrt{\pi} e^{-\xi_a^2} / (\xi_a - \xi_b)(\xi_a - \xi_c)]. \quad (24)$$

The last term of Eq. (24) again gives a Doppler-free spectrum. The two denominators yield, in general, two Lorentzian peaks with halfwidths $(\Gamma_{ij} / \omega_{ij}^0 + \Gamma_{ki} / \omega_{ki}^0)$ and $(\Gamma_{ij} / \omega_{ij}^0 + \Gamma_{mn} / \omega_{mn}^0)$, respectively. They can, however, merge into a single peak as $\xi'_b - \xi'_c$. For the triply resonant processes in Fig. 2 and Eqs. (8) and (9), all except Eq. (8a) should yield Doppler-free spectra. Note that the last term in Eqs. (8c) and (8d) also contributes to the Doppler-free spectra since we can write $2\Gamma_{n'\epsilon} / [(\omega_1 - \omega_{n'\epsilon})^2 + \Gamma_{n'\epsilon}^2] = [(\omega_1 - \omega_{n'\epsilon} - i\Gamma_{n'\epsilon})^{-1} - (\omega_1 - \omega_{n'\epsilon} + i\Gamma_{n'\epsilon})^{-1}]$.

B. Inhomogeneous crystal-field broadening

We consider here ions or molecules in a condensed matter. The energy levels of the ions or molecules are modified by the local potential V due to neighboring ions. This is sometimes known as the crystal-field effect. We can write

$$V = \langle V \rangle + \alpha u_\alpha + \beta u_\beta + \dots, \quad (25)$$

where $\langle V \rangle$ is the average potential and u_α, u_β, \dots are the normalized potentials of various symmetries with their strengths α, β, \dots being random variables subject to the local variation. Then, the eigenenergy of state $|i\rangle$ is a function of α, β, \dots and, in the first-order approximation, can be written as

$$\lambda_i(\alpha, \beta, \dots) = \lambda_i^0 + \alpha \Delta \lambda_{i,\alpha} + \beta \Delta \lambda_{i,\beta} + \dots \quad (26)$$

The resonant transition frequency between states $|i\rangle$ and $|j\rangle$ becomes

$$\omega_{ij}(\alpha, \beta, \dots) = \omega_{ij}^0 + \alpha \Delta \omega_{ij,\alpha} + \beta \Delta \omega_{ij,\beta} + \dots \quad (27)$$

The inhomogeneous broadening results from local variation of the random crystal-field parameters α, β , etc. In the central limit, the distribution

function $g(\alpha, \beta, \dots)$ is a Gaussian

$$\begin{aligned}
g(\alpha, \beta, \dots) &= [(1/\sqrt{\pi} \alpha_0) \exp(-\alpha^2/\alpha_0^2)] \\
&\times [(1/\sqrt{\pi} \beta_0) \exp(-\beta^2/\beta_0^2)] \dots, \quad (28)
\end{aligned}$$

where α_0, β_0, \dots are constants. Finally, Eq. (13) should be used to calculate $\langle X_R^{(3)} \rangle$.

The number of parameters α, β, \dots , required to describe the crystal field can often be large (more than ten in a crystal of lower symmetry). Consequently, the calculation of $\langle X_R^{(3)} \rangle$ averaging over the crystal-field distribution is, in general, extremely difficult even if the constants $\Delta \omega_{ij,\alpha}$, $\Delta \omega_{ij,\beta}, \dots$ in Eq. (27) are known. In some cases, however, one particular term, say αu_α , in the local potential of Eq. (25) may dominate. Then, neglecting the effects of β, γ , etc., we approximate $\omega_{ij}(\alpha, \beta, \dots)$ and $g(\alpha, \beta, \dots)$ by

$$\begin{aligned}
\omega_{ij}(\alpha) &\simeq \omega_{ij}^0 + \alpha \Delta \omega_{ij,\alpha}, \\
g(\alpha) &\simeq (1/\sqrt{\pi} \alpha_0) \exp(-\alpha^2/\alpha_0^2). \quad (29)
\end{aligned}$$

Although the variables are different, these expressions are identical to those in Eqs. (14) and (15) for the Doppler case. Therefore, under this approximation, the previous discussion for the Doppler case can apply equally well to the present case. In particular, it is seen that crystal-field-free spectra can be obtained by some doubly and triply resonant four-wave mixing processes.

We should, of course, remember that Eq. (29) is only an approximation. Thus, the elimination of crystal-field broadening is never perfect if the effects of other crystal-field parameters, β, γ , etc., are taken into account. However, if the crystal-field broadening is mainly due to α , these first-order "crystal-field-free" spectra should still show significant narrowing. Our case here is somewhat similar to the case of laser-induced fluorescence line narrowing which has recently been used to study spectra of ions in solids.¹⁷

IV. OUTPUT FROM RESONANT FOUR-WAVE MIXING

Given the nonlinear polarization, the output of four-wave mixing can be derived from the wave

equation in the usual way. We assume here no pump depletion, slow amplitude variation, and negligible boundary reflection of the generated wave. Let the pump fields be

$$\vec{E}_n = \vec{E}_n(z=0) \exp(i\vec{k}_n \cdot \vec{r} - i\omega_n t), \quad n = 1, 2, 3 \quad (30a)$$

and let the output field along \hat{z} be

$$\vec{E}_s = \vec{E}_s(z) \exp(ik_s z - i\omega_s t). \quad (30b)$$

Then, the amplitude $\vec{E}_s(z)$ obeys the equation

$$|E_{si}(z)| = \left| \mathcal{E}_{si}(0) - \frac{2\pi\omega_s^2}{(\Delta\vec{k} \cdot \hat{z})k_s c^2} \langle \chi_{NR}^{(3)} \rangle_{ijkl} + \langle \chi_R^{(3)} \rangle_{ijkl} \mathcal{E}_{1j} \mathcal{E}_{2k} \mathcal{E}_{3l} (1 - e^{i\Delta\vec{k} \cdot \vec{z}}) \right| e^{-\alpha_s i z}. \quad (32)$$

In the absence of an incoming beam in the output mode, $\mathcal{E}_{si}(0) \approx 0$. The power output per unit area at ω_s and \vec{k}'_s with polarization \hat{i} is given by

$$\mathcal{P}_i(\omega_s, \vec{k}'_s, z) = c [\epsilon'(\omega_s)]^{1/2} |E_{si}(z)|^2 / 2\pi. \quad (33)$$

In the special case where the output field also acts as one of the pump fields, for example, $E_{si} = E_{3i}$, the solution of Eq. (31) takes a different form. Since $\omega_3 = \omega_s$ and $\vec{k}_3 = \vec{k}'_s$, we must have $\omega_1 = -\omega_2$, and the nonlinear susceptibility becomes $\tilde{\chi}^{(3)}(\omega_s = \omega_1 - \omega_1 + \omega_s)$. We also have in this case $\Delta\vec{k} = \vec{k}_1(\omega_1) + \vec{k}_2(\omega_1)$. For $E_{1j}(\omega_1) = E_{2k}^*(\omega_2)$, the real part of Δk will vanish. We then find

$$|E_{si}(z)| = |\mathcal{E}_{si}(0) \exp[g_i(z) - \alpha_s i z]|, \quad (34)$$

$$g_i(z) = \frac{2\pi\omega_s^2}{(\Delta\vec{k} \cdot \hat{z})k_s c^2} \langle \chi_{NR}^{(3)} \rangle_{ijkl} + \langle \chi_R^{(3)} \rangle_{ijkl} \times \mathcal{E}_{1j} \mathcal{E}_{2k} (1 - e^{i\Delta\vec{k} \cdot \vec{z}}).$$

The real part of $g_i(z)$ represents a gain coefficient. For $E_{1j}(\omega_1) = E_{2k}^*(\omega_2)$, and $\langle \chi_{NR}^{(3)} \rangle_{ijkl}$ being purely real, we obtain

$$\text{Re}[g_i(z)] \cong \frac{2\pi\omega_s^2}{(\Delta k'')k_s c^2} \text{Im} \langle \chi_R^{(3)} \rangle_{ijkl} |\mathcal{E}_{1j}|^2 (1 - e^{-\Delta k'' z}). \quad (35)$$

From Eqs. (32) and (34) it is seen that the output of four-wave mixing generally depends on a number of factors. We discuss here the effects of phase mismatch, resonant enhancement of $\tilde{\chi}^{(3)}$ and absorption, and polarization of input and output waves.

A. Phase matching

As in all optical parametric processes, phase matching is of prime importance in four-wave mixing. This is governed as usual by the factor $[1 - \exp(i\Delta\vec{k} \cdot \vec{z})]/(\Delta\vec{k} \cdot \hat{z})$ in Eqs. (32) and (34). At phase matching, $\Delta k' = 0$, it is a maximum equal to

$$\frac{\partial \mathcal{E}_{si}}{\partial z} = \frac{-4\pi\omega_s^2}{i2k_s c^2} \langle \chi^{(3)} \rangle (\omega_s = \omega_1 + \omega_2 + \omega_3)_{ijkl} \mathcal{E}_{1j} \mathcal{E}_{2k} \mathcal{E}_{3l} e^{i\Delta\vec{k} \cdot \vec{z}},$$

$$\Delta\vec{k} = \Delta\vec{k}' + i\Delta\vec{k}'' = (\vec{k}'_1 + \vec{k}'_2 + \vec{k}'_3 - \vec{k}'_s) + i\hat{z}(\alpha_{1j} + \alpha_{2k} + \alpha_{3l} - \alpha_{si}), \quad (31)$$

$$\vec{k}_n = \vec{k}'_n + i\alpha_{ni}(\hat{k}'_n \cdot \hat{z})\hat{k}'_n = [\omega_n \sqrt{\epsilon(\omega_n)} / c] \hat{k}'_n.$$

For simplicity, we have used here the plane wave approximation with the assumption that \vec{k}_s is perpendicular to the boundary surface of the nonlinear medium at $z=0$. The solution of Eq. (31) leads to

$[1 - \exp(-\Delta\vec{k}'' \cdot \vec{z})]/(\Delta\vec{k}'' \cdot \hat{z})$, which reduces to z when $|\Delta\vec{k}'' \cdot \vec{z}| \ll 1$. It reduces in magnitude as $|\Delta k'|$ increases from zero. In the limit of $|\Delta\vec{k}'' \cdot \vec{z}| \ll 1$, this phase-matching peak as a function of $\Delta k'$ has a halfwidth of $\sim \pi/z$. In the limit of $|\Delta\vec{k}'' \cdot \vec{z}| \gg 1$, the halfwidth becomes $\Delta k''$ independent of z . In four-wave mixing, phase matching can be achieved in infinite number of ways by properly adjusting the directions of propagation of the three pump waves. In actual experiment, which phase-matching arrangement is preferred depends on practical consideration, such as optimum beam overlapping length, better spatial discrimination against scattering background, etc. The generated wave amplitude in Eq. (32) or the gain coefficient in Eq. (34) is, of course, a maximum at phase matching.

B. Polarization consideration

The output field of Eq. (32) with $\mathcal{E}_{si}(0) = 0$ can be written in the form

$$\vec{E}_s = A (\langle \tilde{\chi}_{NR}^{(3)} \rangle + \langle \tilde{\chi}_R^{(3)} \rangle) : \vec{E}_1 \vec{E}_2 \vec{E}_3. \quad (36)$$

Thus, given \vec{E}_1 , \vec{E}_2 , and \vec{E}_3 , the polarization of the output field depends on the tensorial properties of $\langle \tilde{\chi}_{NR}^{(3)} \rangle$ and $\langle \tilde{\chi}_R^{(3)} \rangle$, and the output power is proportional to $|\hat{e}_s \cdot (\langle \tilde{\chi}_{NR}^{(3)} \rangle + \langle \tilde{\chi}_R^{(3)} \rangle) : \hat{e}_1 \hat{e}_2 \hat{e}_3|^2$, where \hat{e} 's are the unit polarization vectors. The contributions of $\tilde{\chi}_{NR}^{(3)}$ and $\tilde{\chi}_R^{(3)}$ can, in principle, be separated through their dependences on the pump frequencies, and their tensor elements can be deduced through appropriate polarization arrangement. In some cases, however, $|\langle \tilde{\chi}_{NR}^{(3)} \rangle|$ is much larger than $|\langle \tilde{\chi}_R^{(3)} \rangle|$. Small fluctuations in the output would make the extraction of the dispersive $\langle \tilde{\chi}_R^{(3)} \rangle$ out of the nondispersive $\langle \tilde{\chi}_{NR}^{(3)} \rangle$ background rather difficult. Yet it is the dispersion of $\langle \tilde{\chi}_R^{(3)} \rangle$ we are often interested in finding. To achieve this aim, we must suppress as much as possible the $\langle \tilde{\chi}_{NR}^{(3)} \rangle$ background. This has been demon-

strated with the induced gain or loss spectroscopy¹⁰ [Eq. (34)], or the optical heterodyne detection of the Raman-induced Kerr effect.¹¹ In fact, even in the general case [Eq. (32)], a selective polarization detection of the output may be used to suppress the $\langle \tilde{\chi}_{NR}^{(3)} \rangle$ background.⁷

$$\begin{aligned} \vec{E}_s &= \vec{E}_s^{NR} + \vec{E}_s^R, \\ \vec{E}_s^{NR} &= \hat{e}_\mu (A^{NR} \hat{e}_\mu \cdot \langle \tilde{\chi}_{NR}^{(3)} \rangle : \vec{E}_1 \vec{E}_2 \vec{E}_3), \\ \vec{E}_s^R &= [A_\mu^R \hat{e}_\mu (\hat{e}_\mu \cdot \langle \tilde{\chi}_R^{(3)} \rangle) + A_\nu^R \hat{e}_\nu (\hat{e}_\nu \cdot \langle \tilde{\chi}_R^{(3)} \rangle)] : \vec{E}_1 \vec{E}_2 \vec{E}_3, \end{aligned} \quad (37)$$

$$R = A_\nu^R \hat{e}_\nu \cdot \langle \tilde{\chi}_R^{(3)} \rangle : \hat{e}_1 \hat{e}_2 \hat{e}_3 / [\hat{e}_\mu \cdot (A^{NR} \langle \tilde{\chi}_{NR}^{(3)} \rangle + A_\mu^R \langle \tilde{\chi}_R^{(3)} \rangle) \cdot \hat{e}_1 \hat{e}_2 \hat{e}_3]. \quad (39)$$

If

$$|A^{NR} \hat{e}_\mu \cdot \langle \tilde{\chi}_{NR}^{(3)} \rangle : \hat{e}_1 \hat{e}_2 \hat{e}_3| \gg |A_\mu^R \hat{e}_\mu \cdot \langle \tilde{\chi}_R^{(3)} \rangle : \hat{e}_1 \hat{e}_2 \hat{e}_3|,$$

then we have

$$R \cong (A_\nu^R / A^{NR}) \hat{e}_\nu \cdot \langle \tilde{\chi}_R^{(3)} \rangle : \hat{e}_1 \hat{e}_2 \hat{e}_3 / \hat{e}_\mu \cdot \langle \tilde{\chi}_{NR}^{(3)} \rangle : \hat{e}_1 \hat{e}_2 \hat{e}_3. \quad (40)$$

This ratio now yields a spectrum of $\langle \tilde{\chi}_R^{(3)} \rangle$ normalized against $\langle \tilde{\chi}_{NR}^{(3)} \rangle$. It is independent of the pump fields and therefore in real experiments will be free of trouble caused by the fluctuations of the pump fields.

We note that R is generally complex. In the above arrangement, we will detect $|R|^2$. If, however, the analyzer is rotated by a small angle θ away from \hat{e}_ν , then following Eq. (37) the signal $|R|^2$ is replaced by

$$\begin{aligned} |R_1|^2 &= |\tan \theta + R|^2 \\ &= (\tan \theta + R')^2 + R''^2 \\ &\cong \tan^2 \theta + 2(\tan \theta)R' \quad \text{if } |\tan \theta| \gg |R|, \end{aligned} \quad (41)$$

where $R = R' + iR''$. When a quarter-wave plate is inserted to advance or retard the relative phase of the \hat{e}_ν component by 90° , the signal becomes

$$\begin{aligned} |R_2|^2 &= |\tan \theta \pm iR|^2 \\ &\cong \tan^2 \theta \mp 2(\tan \theta)R'' \quad \text{if } |\tan \theta| \gg |R|. \end{aligned} \quad (42)$$

From Eqs. (41) and (42), we realize that we can obtain R' and R'' from measurements of $|R_1|^2$ and $|R_2|^2$, respectively. If $\langle \tilde{\chi}_{NR}^{(3)} \rangle$ is real, as is often the case, then they allow us to find $\text{Re} \langle \tilde{\chi}_R^{(3)} \rangle$ and $\text{Im} \langle \tilde{\chi}_R^{(3)} \rangle$ separately in terms of $\langle \tilde{\chi}_{NR}^{(3)} \rangle$. This has been proposed and demonstrated in Ref. 7.

C. Absorption and resonant enhancement

Often inherent to resonant four-wave mixing is absorption at pump and/or output frequencies.

where \hat{e}_μ and \hat{e}_ν are orthonormal to each other. Then, by using a polarization analyzer to selectively detect only the \hat{e}_ν polarization component of the output, we obtain, after the analyzer, an output

$$\vec{E}_s = \hat{e}_\nu A_\nu^R (\hat{e}_\nu \cdot \langle \tilde{\chi}_R^{(3)} \rangle) : \vec{E}_1 \vec{E}_2 \vec{E}_3. \quad (38)$$

In this case, the $\langle \tilde{\chi}_{NR}^{(3)} \rangle$ background is completely suppressed. By detecting both \hat{e}_μ and \hat{e}_ν polarization components and taking their ratio, we obtain

Absorption is detrimental to four-wave mixing. It broadens the phase-matching peak, reduces the effective length of interaction, and sometimes makes the deduction of the dispersion of $\tilde{\chi}^{(3)}$ from the observed spectrum less straightforward. Aside from the attenuation factor $\exp(-\alpha_{si}z)$, the effect of absorption on $E_{si}(z)$ in Eq. (32) or on g_i in Eq. (34) is again governed by the factor $[1 - \exp(i\Delta \vec{k} \cdot \vec{z})] / (\Delta \vec{k} \cdot \vec{z})$. We consider here the phase-matching case, $\Delta k' = 0$. This factor then reduces to

$$\mathcal{L} = [1 - \exp(-\Delta k''z)] / \Delta k''. \quad (43)$$

Clearly, the simplest case is when $|\Delta k''z| \ll 1$ so that $\mathcal{L} = z$. This is actually equivalent to saying that the effect of absorption is negligible [aside from the factor $\exp(-\alpha_{si}z)$ mentioned above]. Such a case can happen when (1) all absorption coefficients α_n are sufficiently small, or (2) the interaction length z is sufficiently small, or (3) the four waves form two counterpropagating pairs with $\alpha_{1j} \cong -\alpha_{2k}$ and $\alpha_{3i} \cong -\alpha_{si}$. (In passing, we note that counterpropagating waves in four-wave mixing can have important effects on the Doppler-broadened spectra.) The observed spectrum after normalization against $\mathcal{E}_{1j} \mathcal{E}_{2k} \mathcal{E}_{3i} \exp(-\alpha_{si}z)$ yields the dispersion of $\tilde{\chi}^{(3)}$. [We assume $\mathcal{E}_{si}(0) = 0$ in this section.] Note that in Eqs. (32) and (34), the amplitudes \mathcal{E}_{1j} , \mathcal{E}_{2k} , and \mathcal{E}_{3i} are all taken at $z = 0$. For a pump wave propagating into the nonlinear medium at $z = l$ and leaving the medium at $z = 0$, we have $\mathcal{E} = \mathcal{E}(l) \exp(-\alpha l)$.

In the opposite limit when the attenuation of pump waves is large so that $\Delta k''z \gg 1$, the factor α in Eq. (43) reduces to $(\Delta k'')^{-1}$. Then, aside from the $\exp(-\alpha_{si}z)$ factor, the output amplitude in Eq. (32) or g_i in Eq. (34) becomes independent of z , as one would expect physically. The observed spectrum is proportional to $|\langle \tilde{\chi}_{NR}^{(3)} \rangle_{ijkl} + \langle \tilde{\chi}_R^{(3)} \rangle_{ijkl} / \Delta k''|^2 \exp(-2\alpha_{si}z)$, assuming all pump waves enter the medium at $z = 0$ (or in measuring

the gain, the spectrum of Reg_i is proportional to $\text{Re}[\langle \chi_{\text{NR}}^{(3)} \rangle_{ijkl} + \langle \chi_{\text{R}}^{(3)} \rangle_{ijkl} / \Delta k'']$. Even if the $\langle \chi_{\text{NR}}^{(3)} \rangle$ background can be eliminated by polarization arrangement, it becomes proportional to

$$\begin{aligned} & |\langle \chi_{\text{R}}^{(3)} \rangle_{ijkl} e^{-\alpha_{si} z} / \Delta k''|^2 \\ & = |\langle \chi_{\text{R}}^{(3)} \rangle_{ijkl} e^{-\alpha_{si} z} / (\alpha_{1j} + \alpha_{2k} + \alpha_{3l} - \alpha_{si})|^2. \end{aligned} \quad (44)$$

Thus, in deducing the dispersion of $\chi_{\text{R}}^{(3)}$ from the observed four-wave mixing spectrum, one must have knowledge about the dispersions of α 's. Note that α_{ni} is often only appreciable when ω_n approaches a resonant transition frequency. Therefore, near resonance, the resonant enhancement of the output through $\langle \chi^{(3)} \rangle$ may be partially offset by the presence of resonant absorption. In particular, the absorption at the output frequency should be avoided, if possible, since it leads to a direct exponential attenuation on the output.

Complication of the output spectrum due to absorption can, however, be eliminated with the polarization-sensitive scheme discussed in Sec. IV B. As shown in Eqs. (39) and (40), the ratio R is independent of α 's, and therefore the corresponding output spectrum becomes independent of absorption. This is another great advantage of using the polarization-sensitive scheme for resonant four-wave mixing spectroscopy.

In some cases, α_{si} dominates over the other α 's. If $\alpha_{si} z \gg 1$, the output of Eq. (32) with $\mathcal{E}_{si}(0) = 0$ becomes proportional to $|\langle \chi_{\text{NR}}^{(3)} \rangle_{ijkl} + \langle \chi_{\text{R}}^{(3)} \rangle_{ijkl} \exp[-(\alpha_{1j} + \alpha_{2k} + \alpha_{3l})z] / \alpha_{si}|$. Physically, this means that the output is effectively generated in a section of the order of an attenuation length $1/\alpha_{si}$ at the end of the medium. Again, in the output spectrum, the resonant enhancement of $\tilde{\chi}_{\text{R}}^{(3)}$ is partially offset by the α 's, and in deducing the dispersion of $\tilde{\chi}_{\text{R}}^{(3)}$ from the four-wave mixing spectrum, dispersion of the α 's must be taken into account, or the polarization-sensitive scheme must be used.

V. PHYSICAL EXAMPLES OF RESONANT FOUR-WAVE MIXING

A. General consideration

While different four-wave mixing processes may require different experimental arrangements, a number of general observations can be made, following the discussion in the above section. First of all, our aim is to measure the spectrum of $\tilde{\chi}_{\text{R}}^{(3)}$, but $\tilde{\chi}_{\text{NR}}^{(3)}$ often produces a troublesome background. Extraction of the $\tilde{\chi}_{\text{R}}^{(3)}$ spectrum from the $\tilde{\chi}_{\text{NR}}^{(3)}$ background requires that either $|\tilde{\chi}_{\text{R}}^{(3)}| \gg |\tilde{\chi}_{\text{NR}}^{(3)}|$ or that the selective polarization arrangement (Sec. IV B) should be used to suppress

$\tilde{\chi}_{\text{NR}}^{(3)}$. Otherwise, the nonlinear spectroscopic measurement will not be possible.

Phase matching is of prime importance in four-wave mixing. It not only maximizes the output signal but also yields a highly directional output beam. The latter feature allows spatial filtering of the output to discriminate against the intense pump beams. This is essential especially when the output frequency is not very different from the input laser frequencies. In principle, keeping the phase-matching condition satisfied, the angles between the output and input beams can be made very large, enabling a more effective spatial filtering. In practice, however, because of the finite beam size, larger angles between input and output beams lead to a shorter interaction length. The resultant signal reduction could be compensated by higher input intensity, but then, in many media, the maximum input intensity is limited by the occurrence of other nonlinear optical processes such as self-focusing, nonlinear absorption, optical breakdown, etc. Therefore, in an actual experiment, a particular phase-matching configuration should be chosen such that within the limiting intensity, an optimum signal-to-noise ratio is achieved with the help of spatial filtering. Phase matching is less important if the effective interaction length is limited by absorption.

In doubly and triply resonant four-wave mixing, absorption cannot be avoided, yet it reduces the output and complicates the spectrum, and therefore should be minimized if possible. Too strong an absorption weakens the signal too much and renders the four-wave mixing spectroscopy impossible. Crudely speaking, the effective length of interaction in the presence of absorption is limited by the attenuation length. To minimize the effect of absorption, one would like to use a medium with an actual length much less than the attenuation length and use intense pump beams to obtain a good output signal-to-noise ratio. In practice, the pump intensity is again limited by the occurrence of other detrimental nonlinear processes. One must therefore use a longer medium and struggle for an optimum signal-to-noise ratio. Then, to obtain the dispersion of $\langle \chi_{\text{R}}^{(3)} \rangle$ from the four-wave mixing spectrum, the polarization-sensitive scheme suggested in Sec. IV B should be used to eliminate the effect of absorption.

As a spectroscopic technique, resonant four-wave mixing can yield spectroscopic information about various transitions. It should be most valuable as a tool to probe transitions between excited states, since many such transitions cannot be studied by ordinary absorption or luminescence experiments. Some four-wave mixing processes

can be used to at least partially eliminate inhomogeneous broadening, so that resolution of overlapping inhomogeneously broadened lines becomes possible. In some cases, even the homogeneous linewidth could then be measured. With three input frequencies, the T_1 lifetime of an excited state may also be deduced from the observed spectral linewidth. The aforementioned information is difficult to obtain with other spectroscopic techniques. We shall discuss some of these applications in the following subsections.

B. Doubly resonant four-wave mixing

We will consider here a few applications of the doubly resonant four-wave mixing spectroscopy.

Resonant CARS is probably the most familiar doubly resonant case. It is described by Figs. 1(a) and 1(c) or Eqs. (7a) and (7c). Aside from resonant frequencies, the $\chi_R^{(3)}$ spectrum in this case yields information about the resonant and nonresonant Raman cross sections. In Eq. (7a), for example, the $|\sum_m \langle \dots \rangle|$ term is the nonresonant Raman transition element, the square of which is proportional to the nonresonant Raman cross section; the term $\langle g' | r_k | n \rangle \langle n | r_l | g \rangle / (\omega_1 - \omega_n + i\Gamma_n)$ is the resonant Raman transition element. Then, if the nonresonant Raman cross section is known from spontaneous Raman scattering, we can deduce from $\chi_R^{(3)}$ the resonant Raman cross section. On the other hand, if the resonant one-photon transition matrix elements $\langle g' | r_k | n \rangle$ and $\langle n | r_l | g \rangle$ are known from absorption and luminescence measurements, then we can deduce from $\chi_R^{(3)}$ the nonresonant Raman transition element. Since the damping coefficients in the two resonant denominators of Eqs. (7a) and (7c) have the same sign, no reduction of inhomogeneous broadening is possible in resonant CARS.

The same information on resonant frequencies and transition matrix elements can be obtained by resonant CSRS (coherent Stokes-Raman scattering), described in Figs. 1(f) and 1(g) or Eqs. (7f) and (7g). However, in Eq. (7g) with ω_2 and $\omega_1 - \omega_2$ at resonances, the damping constants in the resonant denominators are of opposite signs, and therefore, in this particular case, a reduction of inhomogeneous broadening should occur (see Sec. III). This allows a more highly resolved spectroscopic study of transition between the excited states $|n\rangle$ and $|g'\rangle$ in Fig. 1(g).

Figures 1(b) and 1(e) can also be called resonant CARS and resonant CSRS, respectively. With the prescribed double resonances, the transition frequency between the excited states $|n\rangle$ and $|n'\rangle$ can be determined. Then, if the one-photon transition matrix elements from $|g\rangle$ to $|n\rangle$ and from $|g\rangle$ to

$|n'\rangle$ are known from absorption measurements, the nonresonant Raman cross section between $|n\rangle$ and $|n'\rangle$ can be deduced. No reduction of inhomogeneous broadening is possible in these cases. However, if the transition is homogeneously broadened, then these processes yield the damping parameter $\Gamma_{nn'}$ which is difficult to obtain by other means.

The same information about Raman transition between $|n\rangle$ and $|n'\rangle$ can be obtained from processes in Figs. 1(d) and 1(h) or Eqs. (7d) and (7h). In these cases, however, reduction of inhomogeneous broadening should occur and allow a better resolved spectroscopic study on transition between $|n\rangle$ and $|n'\rangle$.

Only two frequencies are involved in the processes in Figs. 1(i) and 1(j), and one of them is solely responsible for the double resonances. As a result, little spectroscopic information, aside from what is already known from linear optical measurements, can be deduced from these processes in steady-state operation. Physically, Fig. 1(i) involves a population change induced by the resonant pumping, which is then probed by a nonresonant beam. A spatial grating can be created if two ω_1 beams are present. Four-wave mixing then corresponds to nonresonant scattering of the probe beam from the induced grating. On the other hand, a birefringence can be induced in the medium if only one ω_1 beam is present. Four-wave mixing in this case corresponds to the probing of the induced birefringence by a nonresonant beam. This last case is often known as the resonant optical Kerr effect. We note that the resonant Kerr effect here involves a doubly resonant $\chi_R^{(3)}$, while the well-known Raman-induced Kerr effect¹⁸ (RIKE) involves only a singly resonant $\chi_R^{(3)}$. In actual experiments, these processes are often complicated by population redistribution in other levels through relaxation as governed by Eq. (4), and the measured $\chi_R^{(3)}$ will not be simply described by Eq. (7i). A very special case involves a fast relaxation of the excitation energy into local heat. A thermal grating can then be induced if two ω_1 beams intersect each other. Scattering of the probe beam by the thermal grating is generally known as forced Rayleigh scattering.¹⁹ With pulsed excitation and delayed probing, the population relaxation and diffusion of the thermal grating can be studied, but we shall not dwell on transient effects in this paper. The process in Fig. 1(j) simply describes the perturbing effect of the nonresonant field on the resonant transition. While these processes seem less interesting here, they become more attractive when the nonresonant field approaches resonance in the triply resonant cases.

C. Saturation spectroscopy and polarization spectroscopy

The induced population change in a certain energy state can be selectively probed by a resonant transition. In an inhomogeneously broadened system, the induced population change by a monochromatic laser excitation is a hole-burning effect. Then the resonant probing should yield a spectrum with reduced inhomogeneous broadening. This is now a well-known high-resolution spectroscopic technique. If induced gain or loss is measured, it is known as the saturation spectroscopy,⁶ and if induced birefringence is probed, it is known as the polarization spectroscopy.²⁰ Thus, for example, in Figs. 2(b) and 2(d), the induced polarization change in the ground state is probed, and a high-resolution spectrum for the $|g\rangle - |n\rangle$ or $|g\rangle - |n'\rangle$ transition can be obtained. In Fig. 2(c), the induced population change in the excited state $|n'\rangle$ is probed, and the high-resolution spectrum of the $|n'\rangle - |g'\rangle$ transition can be obtained.

However, the expressions of $\chi_R^{(3)}$ in Eqs. (8b)–(8d) for Figs. 2(b)–2(d) show that aside from the contribution due to induced population change (the term involving T_1) there is also a contribution from coherent four-wave mixing (the term independent of T_1). The latter should also yield a spectrum with reduced inhomogeneous broadening, as seen from the signs of the damping constants in the resonant frequency denominators. Therefore, the observed high-resolution spectrum is actually a superposition of two lines. Only when T_1 is much larger than $T_2 = \Gamma^{-1}$ can we neglect the coherent mixing contribution.

We realize that induced gain or induced birefringence measurement is not the only way to study the processes in Figs. 2(b)–2(d). The same processes can be studied with the usual four-wave mixing configuration generating a spatially separable output beam in the phase-matching direction. However, in this case, care must be taken to

avoid the effect due to induced thermal grating which arises from relaxation of the excitation energy into local heat.

We also realize that through relaxation, other levels which are not being directly pumped may take on a population change. Resonant transitions from such levels can therefore also be probed. If the intrasystem relaxation is much faster than the intersystem relaxation (i.e., diffusion of the burned hole across the inhomogeneously broadened line), then the observed spectrum should again exhibit a reduced inhomogeneous broadening. This generalization of saturation and polarization spectroscopy may find applications in high-resolution spectroscopic studies, especially in condensed matter.

Incidentally, we note that resonant RIKE (Raman-induced Kerr effect) belongs to the category of polarization spectroscopy and is described by the process in Fig. 2(c) or Eq. (8c).

D. Measurements of T_1

As we mentioned earlier in Sec. II C, the spectrum of four-wave mixing with three input frequencies can be used to obtain the T_1 lifetimes. Physically, two input beams with frequencies ω_1 and ω'_1 near a resonance can induce a population change oscillating at the frequency $\omega_1 - \omega'_1$ with an amplitude proportional to $[(\omega_1 - \omega'_1) + i/T_1]^{-1}$. The induced population change in a particular state can then be probed by a resonant transition from the state, and the resulting spectrum as a function of $(\omega_1 - \omega'_1)$ yields T_1 .

Let us consider the process described by Eq. (9a) as an example. We first consider the case of $T_1\Gamma \gg 1$. We are interested in the variation of $\chi_R^{(3)}(\omega'_2)$ as $(\omega_1 - \omega'_1)$ scans over 0. Then, Eq. (9a) shows that the term involving $T_{1n'}$ arising from an induced population in $|n\rangle$ is mainly responsible for the spectral variation of $\chi_R^{(3)}$. This term after averaging over the inhomogeneous broadening can be written as

$$\langle \chi_{RR}^{(3)}(\omega'_2 = \omega'_1 - \omega_1 + \omega_2) \rangle_{ijkl} = \frac{Ne^4}{\hbar^3} \langle g' | r_i | n \rangle \langle n' | r_j | g \rangle \langle g' | r_k | n' \rangle \langle n' | r_l | g' \rangle \frac{\rho_{gg}^0}{(\omega_1 - \omega'_1 + i/T_{1n'})} \\ \times \int (d\alpha d\beta, \dots) \frac{g(\alpha, \beta, \dots)}{\omega'_2 - \omega_{n'g} + i\Gamma_{n'g}} \left(\frac{1}{\omega_1 - \omega_{n'g} - i\Gamma_{n'g}} - \frac{1}{\omega_1 - \omega_{n'g} + i\Gamma_{n'g}} \right). \quad (45)$$

If $T_{1n'} \gg \Gamma_{n'g}^{-1}$, $\Gamma_{n'g}^{-1}$, the integral in the above equation is practically independent of ω'_1 in the range of $|\omega_1 - \omega'_1| \sim T_{1n'}^{-1}$, and therefore we have

$$\langle \chi_{RR}^{(3)}(\omega'_2) \rangle \propto (\omega_1 - \omega'_1 + i/T_{1n'})^{-1}. \quad (46)$$

Thus, the spectrum of $\langle \chi_{RR}^{(3)}(\omega'_2) \rangle$ vs ω'_1 should yield

a value for $T_{1n'}$. We also note that when ω_1 and ω'_2 are at resonances, the integral in Eq. (45) actually yields a doubly resonant line with reduced inhomogeneous broadening. This means that $\langle \chi_{RR}^{(3)}(\omega'_2) \rangle$ can be sharply enhanced when the probe frequency ω_2 approaches resonance. In other words, the induced population in $|n\rangle$ can now be

selectively probed by the resonant probing. This is important since in practice a large number of states can be populated through relaxation and they can all contribute to $\langle \chi_{RR}^{(3)} \rangle$.

$$\langle \chi_{RR}^{(3)}(\omega'_2 = \omega'_1 - \omega_1 + \omega_2) \rangle_{ijkl} = \frac{Ne^4}{\hbar^3} \frac{\langle n' | r_i | g \rangle \langle g | r_k | n' \rangle}{\omega_1 - \omega'_1 + i/T_{1n'}} \rho_{gg}^0$$

$$\times \sum_m \frac{\gamma_{mn'} \langle g' | r_i | m \rangle \langle m | r_j | g' \rangle}{\omega_1 - \omega'_1 + i/T_{1m}} \int (d\alpha d\beta, \dots) \frac{g(\alpha, \beta, \dots)}{\omega'_2 - \omega_{mg'} + i\Gamma_{mg'}}$$

where for $m = n'$, we have $\gamma_{n'n'} = \omega_1 - \omega'_1 + i/T_{1n'}$. The above equation reduces to Eq. (45) only when all terms with $m \neq n'$ can be neglected. This may happen when $\omega'_2 \approx \omega_{n'g'}$. On the other hand, if $\omega'_2 \approx \omega_{mg'}$, then the particular term relating to $\rho_{mm}^{(2)}$ is resonantly enhanced. Again, the resonant enhancement can be sharp and strong since at the double resonance of $\omega_1 \approx \omega_{n'g'}$ and $\omega'_2 \approx \omega_{mg'}$, the integral in Eq. (47) yields a line with reduced inhomogeneous broadening. This is the four-wave mixing process described in Fig. 3. From Eq.

If we assume that through relaxation a state $|m\rangle$ becomes populated by $\rho_{mm}^{(2)}$ given in Eq. (12), then the more rigorous expression of $\langle \chi_R^{(3)} \rangle$ taking into account $\rho_{mm}^{(2)}$ using Eq. (11) should be

$$\times \left(\frac{1}{\omega_1 - \omega_{n'g'} - i\Gamma_{n'g'}} - \frac{1}{\omega_1 - \omega_{n'g'} + i\Gamma_{n'g'}} \right), \quad (47)$$

(47) we expect that the spectrum of $\langle \chi_R^{(3)}(\omega'_2) \rangle$ vs ω'_1 could yield T_{1m} if we selectively tune ω_2 to various resonances.

If $T_1\Gamma \sim 1$, the spectrum is more complicated. We assume here that the inhomogeneous broadening can be described by a Gaussian distribution of Eq. (29) with a single parameter. Then using the calculation developed in Sec. III A, and neglecting the weakly dispersive part, we obtain the average of Eq. (9a) as

$$\langle \chi_R^{(3)}(\omega'_2 = \omega_1 - \omega'_1 + \omega_2) \rangle_{ijkl} = \int d\alpha g(\alpha) [\chi_R^{(3)}(\omega'_2)]_{ijkl}$$

$$\propto \left\{ \frac{\omega_{n'g'}}{\omega_{n'g'}(\omega_{n'g'}^0 + \omega_{n'g'}^0)} \left[(\omega_1 - \omega'_1) + s_2 - \frac{\omega_{n'g'}^0}{\omega_{n'g'}^0} s_1 + i \left(\frac{\omega_{n'g'}^0}{\omega_{n'g'}^0} \Gamma_{n'g'} + \frac{\omega_{n'g'}^0}{\omega_{n'g'}^0} \Gamma_{n'g'} \right) \right]^{-1} \right.$$

$$\times \left. \left((\omega_1 - \omega'_1) + \frac{\omega_{n'g'}^0 s_2 - \omega_{n'g'}^0 s_1 + i(\omega_{n'g'}^0 \Gamma_{n'g'} + \omega_{n'g'}^0 \Gamma_{n'g'})}{\omega_{n'g'}^0 + \omega_{n'g'}^0} \right)^{-1} \right.$$

$$\left. + \frac{1}{\omega_{n'g'}^0 (\omega_1 - \omega'_1 + i/T_{1n'})} \left[(\omega_1 - \omega'_1) + s_2 - \frac{\omega_{n'g'}^0}{\omega_{n'g'}^0} s_1 + i \left(\Gamma_{n'g'} + \frac{\omega_{n'g'}^0}{\omega_{n'g'}^0} \Gamma_{n'g'} \right) \right]^{-1} \right\}, \quad (48)$$

where $s_1 = \omega_1 - \omega_{n'g'}^0$ and $s_2 = \omega_2 - \omega_{n'g'}^0$. Since $T_1\Gamma \sim 1$, the doubly resonant denominators in the above equation as $\omega'_1 - \omega_1$ complicate the spectrum. However, with three input frequencies, we have the freedom to choose s_1 and s_2 , aside from choosing ω'_1 as the scanning frequency. For example, we can let $s_1 = 0$ and $s_2 = 2\Gamma_{n'g'}$. Then, as ω'_1 approaches ω_1 , only the $(\omega_1 - \omega'_1 + i/T_{1n'})^{-1}$ term is at resonance; the other denominators simply contribute a sloping background and somewhat distort the resonant lineshape. The lifetime $T_{1n'}$ can again be deduced from the resonant linewidth.

We note that in the actual experiment, another output beam at $\omega''_2 = \omega_1 - \omega'_1 + \omega_2$ should be simultaneously created with $\langle \chi_R^{(3)}(\omega''_2) \rangle$ obtained by interchanging ω_1 and ω'_1 in $\langle \chi_R^{(3)}(\omega'_2 = \omega'_1 - \omega_1 + \omega_2) \rangle$. The two output beams at ω'_2 and ω''_2 may interfere, but they can be separated through phase matching with

appropriate wave-vector arrangement.

Measurements of T_1 and T_2 using four-wave mixing spectroscopy with two input frequencies have been proposed and demonstrated by Yajima *et al.*⁸ Because of the lack of a third adjustable input frequency for selective resonant probing, the experiment has little flexibility and the interpretation of the results is less straightforward.

E. Distinction between resonant Raman scattering and resonant emission

Recently, the problem of distinguishing resonant Raman scattering and hot luminescence has received a great deal of attention.⁹ From the physical point of view, the two processes are different in the sense that Raman scattering involves only transverse excitation with T_2 relaxation times while luminescence involves a longitudinal pumping with a real population change and a T_1 relaxa-

tion time. In practice, however, it is difficult to resolve the two in the spontaneous spectrum, although they may be distinguishable from time-dependent measurements.

As we know, both resonant Raman scattering and hot luminescence have their counterparts in four-wave mixing. Resonant Raman scattering corresponds to a coherent triply resonant four-wave mixing process involving only transverse excitation. Hot luminescence corresponds to a triply resonant four-wave mixing process involving a longitudinal pumping of population to an excited state followed by a resonant probing at an emission frequency. (We call this a resonant emission process.) Thus, just as in the case of light scattering, although Fig. 2(c) appears to describe a single four-wave mixing process, it actually consists of both coherent resonant Raman scattering and resonant emission. This is explicitly shown by the two separate terms in Eq. (8c). Again, it will be difficult to resolve the two parts in the overall four-wave mixing spectrum, although we know that if $T_1 \gg \Gamma_{n'g}^{-1}$, the resonant emission part should dominate. Both the coherent Raman process and the resonant emission in Eq. (8c) have a reduced inhomogeneous broadening. On the other hand, if ω_1 instead of ω_2 is the output frequency as described by Fig. 2(a) or Eq. (8a), then the process becomes purely coherent Raman and can be called a resonant inverse Raman process. However, this process does not have a reduced inhomogeneous broadening. It has a strength ratio of $\sim \Gamma_{n'g'}/\Gamma_{n'g}$ compared with the coherent part of Eq. (8c).

With three input frequencies in the triply resonant four-wave mixing, Eq. (8c) changes over to Eq. (9a). It can be seen clearly from Eq. (9a) that the coherent Raman process now has a very different spectrum as a function of $(\omega_1 - \omega'_1)$ from the resonant emission. Thus, the triply resonant four-wave mixing of Eq. (9a) provides a unique method which can unambiguously resolve the contribution of resonant Raman scattering and resonant emission in a single process.

VI. EXPERIMENTAL CONSIDERATIONS

A characteristic advantage of nonlinear spectroscopic techniques is that the absolute intensity of the signal is fairly large. This means that usually it is not necessary to use low-signal detection systems such as photon counting. Usually, low-gain photomultipliers or even photodiodes are sensitive enough to detect the nonlinear signal. However, the sensitivity is actually limited by various sources of noise, due to some other light coming onto the detector, which constitutes a

fluctuating background superimposed on the resonant signal. This problem has recently received considerable attention and several new schemes have been proposed to reduce this background and improve the signal-to-noise ratio. We discuss in this section various types of background as well as some experimental arrangements that improve the sensitivity.

A. Discrimination against incoherent background

In four-wave mixing experiments, scattered light and/or luminescence from the sample are often present and some care must be taken to discriminate against them. Since the nonlinear signal is a coherent beam this discrimination can be relatively easy through spatial and frequency filtering, except in unfavorable cases. Time resolution and polarization selection may provide additional discrimination against such noise background. For example, the use of pulsed lasers and gated electronics ensures a very effective time discrimination against background light or luminescence with long lifetime as in the cases of flame and plasma studies.

Frequency discrimination is most conveniently performed through a monochromator, with the help of interference filters. In many cases a double monochromator is preferred because of its high rejection ratio. Very often the spectral resolution of the experiment is provided by the laser linewidths. Then, the resolution of the monochromator can be low so that it can easily track the signal frequency in synchronism with the frequency scan of the input laser. Another experimental scheme uses a broadband continuum source as one of the incident beams.²¹ The resulting signal can be recorded by a spectrograph or by an optical multichannel analyzer. The advantage is that the signal spectrum can be virtually obtained on a one-shot basis. However, a very smooth continuum is required if high resolution and sensitivity are expected.

Spatial discrimination is most effective when the signal beam has a low divergence. A good transverse-mode structure (ideally Gaussian TEM₀₀) of the incident beams helps in this respect. Two apertures are needed to provide a complete spatial selection, one in the near field and one in the far field. When the input beams are focused on the sample (Rayleigh range shorter than 10 cm), the easiest way is to put an aperture at some distance from the sample to provide the far-field selection. The signal beam is then refocused onto a pinhole or the entrance slit of a monochromator, which provides the second aperture. When the input beams are not focused (e.g., in the case of

high peak power), the far field can be selected by an aperture placed in the focal plane of a converging lens. Special geometries have been suggested to improve the discrimination against elastically scattered light.²² This is especially important when the signal frequency is so close to one of the input frequencies that the frequency discrimination is ineffective (e.g., in detection of acoustic²³ or low-frequency Raman modes). For instance, counterpropagating pump and probe beams can be used in RIKE or stimulated Raman gain spectroscopy.²³ Phase matching may be set up to allow large angles between the interacting beams,²² but one then needs incoming beams with fairly high peak power and small divergence, because the large crossing angles reduce the interaction volume.

B. Suppression of nonresonant background by polarization arrangement

As discussed in Sec. IV B, the polarization-sensitive detection scheme allows discrimination against the nonresonant background $\chi_{NR}^{(s)}$, a separate determination of the real and imaginary parts of $\chi_R^{(s)}$, and the reduction of the effects of absorption and laser intensity fluctuations. It also improves significantly the signal-to-noise ratio as we shall see later. A typical experimental arrangement is shown in Fig. 4. Each input beam must be in a pure state of polarization when reaching the sample to ensure a good extinction ratio for the nonlinear output beam after the analyzer—a ratio of 10^{-4} to 10^{-5} may be obtained with some care on good optical quality samples. An adjustable retardation plate between the sample and the analyzer may help to compensate for residual birefringence in the sample, focusing optics or cell windows.

Two photodetectors monitor simultaneously the two polarization components separated by the analyzer. The ratio of the two output signals provides a normalized quantity, characteristic of the polarization state of the nonlinear output wave but insensitive to the laser intensity fluctuations. To analyze different polarization states of the output, it is preferable to use a polarization rotator (half-wave birefringent plate or double Fresnel rhomb) in front of the fixed analyzer instead of rotating the analyzer. Since the monochromator for selecting the signal frequency may depolarize the beam and spoil the extinction ratio, the analyzer should be in front of the input slit. The two analyzed components can be focused on different parts of the slit. They are then spatially separated at the exit slit, and can be separately detected by the two photodetectors.

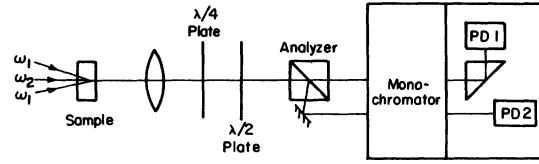


FIG. 4. Possible experimental arrangement for polarization-sensitive four-wave mixing spectroscopy.

C. Signal-to-noise ratio with pulsed lasers

Several authors have recently discussed the signal-to-noise (S/N) ratio in stimulated Raman gain spectroscopy,¹⁰ optical heterodyne detection of nonlinear spectroscopy,¹¹ and Raman spectroscopy in gases.¹⁰ We consider here the improvement in the S/N ratio when using the polarization-sensitive technique just described. We restrict the discussion to the case of pulsed lasers.

We assume that the four-wave mixing output is large enough so that the shot-noise is negligible compared to the classical noise due to intensity and mode fluctuations of the input beams. In addition, we assume that the stray light can also be reduced to a negligible level. With high peak power lasers, these conditions can often be met in practice, and the ultimate limit for the detection of weak resonances is determined by the fluctuating background at the detector. We consider and compare here the signal-to-noise ratios of three different but related cases: (1) ordinary four-wave mixing without polarization selection, (2) measurement of $|\chi_R^{(s)}/\chi_{NR}^{(s)}|$ with background suppression of $\chi_{NR}^{(s)}$ by polarization selection, and (3) measurement of $\text{Re}(\chi_R^{(s)}/\chi_{NR}^{(s)})$ and $\text{Im}(\chi_R^{(s)}/\chi_{NR}^{(s)})$ with polarization selection.

(1) *Ordinary four-wave mixing.* In going through a weak resonance ($|\chi_R^{(s)}| \ll |\chi_{NR}^{(s)}|$), the resonant signal has a relative variation $\langle \Delta I_R \rangle / \langle I_{NR} \rangle$ with respect to the nonresonant background due to $\chi_{NR}^{(s)}$,

$$\frac{\langle \Delta I_R \rangle}{\langle I_{NR} \rangle} = \frac{|\chi_R^{(s)} + \chi_{NR}^{(s)}|^2 - |\chi_{NR}^{(s)}|^2}{|\chi_{NR}^{(s)}|^2} \approx \frac{2\chi_R'}{\chi_{NR}^{(s)}}, \quad (49)$$

where $\chi_R^{(s)} = \chi_R' + i\chi_R''$ and $\chi_{NR}^{(s)}$ is assumed to be real. This is to be compared with the fluctuations in the nonresonant background relative to the average background

$$\mathcal{G}_1 = \langle \delta I_{NR}^2 \rangle^{1/2} / \langle I_{NR} \rangle. \quad (50)$$

If each data point is taken by averaging over N_p shots, the background fluctuations are reduced by a factor of $\sqrt{N_p}$. Then, the effective signal-to-noise ratio is

$$\frac{S}{N} = \frac{\langle \Delta I_R \rangle \sqrt{N_p}}{\mathcal{G}_1 \langle I_{NR} \rangle} \approx \frac{2\sqrt{N_p} \chi_R'}{\mathcal{G}_1 \chi_{NR}^{(s)}}. \quad (51)$$

(2) *Background suppression by polarization selection.* The normalized resonant signal at the detector in this case is $|R|^2$ with R given by Eq. (38) or (39). The background of the resonant spectrum here is due to the finite extinction coefficient η of the analyzer. The signal relative to the background is $|R|^2/\eta$. The fluctuations in the background now arise from relative fluctuations and nonlinearities in the two detection channels, and can be designated as $\mathcal{E}_2/\sqrt{N_p}$. Thus, the signal-to-noise ratio is

$$\frac{S}{N} = \frac{|R|^2\sqrt{N_p}}{\eta\mathcal{E}_2}. \quad (52)$$

(3) *Measurements of $\text{Re}(\chi_R^{(3)})$ and $\text{Im}(\chi_R^{(3)})$.* Following Eq. (41), for example, the normalized resonant signal is $2(\tan\theta)R'$, and the background is $\tan^2\theta + \eta$, where η is again the extinction ratio of the analyzer. The signal relative to the background becomes $2(\tan\theta)R' / (\tan^2\theta + \eta)$. With $\mathcal{E}_2/\sqrt{N_p}$ being the background fluctuations, the signal-to-noise ratio is given by

$$\frac{S}{N} = \frac{2(\tan\theta)R'\sqrt{N_p}}{\mathcal{E}_2(\tan^2\theta + \eta)} \quad (53)$$

which has a minimum at $\tan\theta \simeq \theta = \sqrt{\eta}$.

As a numerical example, we consider four-wave mixing in an isotropic medium with, for instance, $R = \chi_R'/2\chi_{NR}$. We assume typical values of $\mathcal{E}_1 = 0.1$, $\mathcal{E}_2 = 0.01$, $\eta = 10^{-5}$, $\theta^2 = 10^{-5}$, and $N_p = 100$. Then, we find for $S/N = 1$ in the three cases the detection limit of

$$|\chi_R'/\chi_{NR}^{(3)}| = \begin{cases} 5 \times 10^{-3} \\ 2 \times 10^{-4} \\ 6 \times 10^{-6} \end{cases}$$

for the three respective cases. Case (3) is therefore the most sensitive way to detect a weak resonance. It leads to an improvement of 3 orders of magnitude in sensitivity over the ordinary case.

It is interesting to note the close analogy between the present case and the simpler case of stimulated Raman gain spectroscopy.^{10,11} The intensity variation of the probe beam due to the Raman gain is similar to case (1).¹⁰ The Raman-induced Kerr effect is the polarized version¹⁸ as in case (2), and its optical heterodyning scheme

as in case (3).¹¹ The main difference is that the local oscillator is provided here by the nonresonant background, instead of the probe beam in the Raman gain experiment.

VII. CONCLUSION

We have considered in this paper the various aspects of doubly and triply four-wave mixing processes. Emphasis is on the potential applications of four-wave mixing as a spectroscopic technique. Explicit expressions for the resonant nonlinear susceptibilities are derived. It is then shown that with double and triple resonances, four-wave mixing can yield high-resolution spectra with reduced inhomogeneous broadening. Unlike the usual spectroscopic techniques, multiresonant four-wave mixing allows us to probe the spectroscopic details of transitions between excited states, to measure the longitudinal relaxation times, and to distinguish resonant Raman scattering from resonant fluorescence. A number of factors possibly affecting the output signal are considered. In particular, an experimental arrangement using the selective polarization scheme is discussed in detail. The normalized polarization-sensitive output effectively suppresses the background due to the nonresonant part of the nonlinear susceptibility. It also greatly reduces the detrimental effects of absorption and laser intensity fluctuations, and can enhance the signal-to-noise ratio by three orders of magnitude in comparison with the ordinary scheme of four-wave mixing.

More complicated cases of multiresonant four-wave mixing have been avoided in the present work. Thus, nonlinear absorption is assumed negligible, compound relaxation processes are not considered, and complex geometry and boundary conditions are not treated. Inclusion of these factors in our description requires special treatment for special cases. Finally, a separate class of interesting problems we have not considered in this paper is on transient resonant four-wave mixing processes. This will be the subject of our next investigation.

This work was supported by the Division of Materials Sciences, Office of Basic Energy Sciences, U. S. Department of Energy under Contract No. W-7405-ENG-48.

*Permanent address: Centre National d'Etudes des Telecommunications, Département RPM, 196, rue de Paris, 92220 Bagneux, France.

¹P. D. Maker and R. W. Terhune, Phys. Rev. A **137**, 801 (1965).

²See, for example, review articles on the subject by S. A. Akhmanov, in *Nonlinear Spectroscopy*, Proceedings of International School of Physics "Enrico Fermi," edited by N. Bloembergen (North-Holland, Amsterdam, 1977), p. 217; W. M. Tolles, J. W. Nibler, J. R. Mc-

- Donald, and G. V. Knighton, in *Topics in Current Physics*, edited by A. Weber (Springer, Berlin, 1977); A. B. Harvey, J. R. McDonald, and W. M. Tolles, in *Progress in Analytical Chemistry* (Plenum, New York, 1977), p. 211; M. D. Levenson, *Physics Today* **30**, 45 (1977); S. Druet and J. P. Taran, in *Chemical and Biochemical Applications of Lasers*, edited by C. B. Moore (Academic, New York, 1979), Vol. IV; N. Bloembergen in *Laser Spectroscopy IV*, edited by H. Walther and K. W. Rothe (Springer, Berlin, 1979), p. 340.
- ³See, for example, R. M. Martin and L. M. Falicov, in *Light Scattering in Solids*, edited by M. Cardona (Springer, New York, 1975), p. 79; P. P. Shoviygin, *Russ. Chem. Rev. (Uspekhi Khimii)* **47**, 907 (1978).
- ⁴I. Chabay, G. K. Klauminzer, and B. S. Hudson, *Appl. Phys. Lett.* **28**, 27 (1976); R. T. Lynch, H. Lotem, and N. Bloembergen, *J. Chem. Phys.* **66**, 4250 (1977); S. A. J. Druet, B. Attal, T. K. Gustafson, and J.-P. E. Taran, *Phys. Rev. A* **18**, 1529 (1978); B. Aital, O. O. Snapp, and J.-P. E. Taran, *Optics Commun.* **24**, 77 (1978); A. Lau, M. Pfeiffer, and W. Werneke, *ibid.* **23**, 59 (1977).
- ⁵S. A. J. Druet, J.-P. E. Taran, and Ch. J. Bordé, *J. Phys. (Paris)* **40**, 841 (1979). Doppler broadening in Raman gain spectroscopy has been investigated by M. Feld and A. Javan, *Phys. Rev.* **177**, 540 (1969); T. Hansch and P. Toschek, *Z. Phys.* **236**, 213 (1970); S. A. J. Druet, J.-P. E. Taran, and Ch. J. Bordé, *J. Phys. (Paris)* **41**, 183 (1980).
- ⁶See, for example, V. S. Letokhov and V. P. Chebotayev, *Nonlinear Laser Spectroscopy* (Springer, Berlin, 1977).
- ⁷S. A. Akhmanov, A. F. Bunkin, S. G. Ivanov, and N. I. Koroteev, *Pis'ma Zh. Eksp. Teor. Fiz. [JETP Lett.]* **25**, 46 (1977); **47**, 667 (1978); J.-L. Oudar, R. W. Smith, and Y. R. Shen, *Appl. Phys. Lett.* **34**, 758 (1979); N. I. Koroteev, M. Endemann, and R. L. Byer, *Phys. Rev. Lett.* **43**, 398 (1979); L. A. Rahn, L. J. Zych, and P. L. Mattern, *Optics Commun.* **30**, 249 (1979).
- ⁸T. Yajima and H. Souma, *Phys. Rev. A* **17**, 309 (1978); T. Yajima, H. Souma, and Y. Ishiba, *ibid.* **17**, 324 (1978); J. J. Song, J. H. Lee, and M. D. Levenson, *ibid.* **17**, 1439 (1978).
- ⁹M. V. Klein, *Phys. Rev. B* **8**, 919 (1973); Y. R. Shen, *Phys. Rev. B* **9**, 622 (1973); **14**, 1772 (1976); J. R. Solin and H. Merkelo, *ibid.* **12**, 624 (1975); D. L. Rousseau, G. D. Patterson, and P. F. Williams, *Phys. Rev. Lett.* **34**, 1306 (1975).
- ¹⁰A. Owyong, *Optics Commun.* **22**, 323 (1977); *IEEE J. Quantum Electron.* **QE-14**, 192 (1978); A. Owyong and E. D. Jones, *Optics Lett.* **1**, 152 (1977); A. Owyong in *Laser Spectroscopy IV*, edited by H. Walter and K. W. Rothe (Springer, Berlin, 1979), p. 175.
- ¹¹J. J. Song, G. L. Easley, and M. D. Levenson, *Appl. Phys. Lett.* **29**, 567 (1976); J. J. Song, G. L. Easley, M. D. Levenson, and W. M. Tolles, *IEEE J. Quantum Electron.* **QE-14**, 45 (1978); M. D. Levenson and G. L. Easley, *Appl. Phys.* **19**, 1 (1979).
- ¹²N. Bloembergen and Y. R. Shen, *Phys. Rev.* **133**, A37 (1964); N. Bloembergen, *Nonlinear Optics* (Benjamin, New York, 1965).
- ¹³N. Bloembergen, H. Lotem, and R. T. Lynch, *Indian J. Pure Appl. Phys.* **16**, 151 (1978); R. T. Lynch, H. Lotem, and N. Bloembergen, *J. Chem. Phys.* **66**, 4250 (1977).
- ¹⁴S. Y. Yee, T. K. Gustafson, S. A. J. Druet, and J.-P. E. Taran, *Optics Commun.* **23**, 1 (1977); T. K. Yee and T. K. Gustafson, *Phys. Rev. A* **18**, 1597 (1978).
- ¹⁵S. Chandra, A. Compaan, and E. Wiener-Avneer, *Appl. Phys. Lett.* **33**, 867 (1978).
- ¹⁶B. D. Fried and S. D. Conte, *The Plasma Dispersion Function* (Academic, New York, 1961).
- ¹⁷A. Szabo, *Phys. Rev. Lett.* **25**, 924 (1970); **27**, 323 (1971); R. Flach, D. S. Hamilton, P. M. Selzer, and W. M. Yen, *Phys. Rev. Lett.* **35**, 1034 (1975).
- ¹⁸D. Heiman, R. W. Hellwarth, M. D. Levenson, and G. Martin, *Phys. Rev. Lett.* **36**, 189 (1976).
- ¹⁹H. Eichler, G. Salje, and H. Stahl, *J. Appl. Phys.* **44**, 5383 (1973).
- ²⁰C. Wieman and T. W. Hansch, *Phys. Rev. Lett.* **36**, 1170 (1976).
- ²¹W. B. Roh, P. W. Schreiber, and J.-P. E. Taran, *Appl. Phys. Lett.* **29**, 174 (1976).
- ²²A. C. Eckbreth, *Appl. Phys. Lett.* **32**, 421 (1978); S. Chandra, A. Compaan, and E. Wiener-Avneer, *Appl. Phys. Lett.* **33**, 867 (1978); A. Compaan and S. Chandra, *Optics Lett.* **4**, 170 (1979); G. Laufer and R. B. Miles, *Optics Commun.* **28**, 250 (1979).
- ²³A. G. Jacobson and Y. R. Shen, *Appl. Phys. Lett.* **34**, 464 (1979).